

PREPARED FOR SUBMISSION TO JHEP

# The $W\gamma$ decay of the elusive charged Higgs boson in the two-Higgs-doublet model with vectorlike fermions

---

Jeonghyeon Song, and Yeo Woong Yoon

*Department of Physics, Konkuk University, Seoul 05029, Korea*

*E-mail:* [jhsong@konkuk.ac.kr](mailto:jhsong@konkuk.ac.kr), [ywoon@kias.re.kr](mailto:ywoon@kias.re.kr)

**ABSTRACT:** The LHC search strategy for the charged Higgs boson  $H^\pm$  in a two-Higgs-doublet model crucially depends on the top quark physics: for the low mass region,  $H^\pm$  is mainly produced from the decay of a top quark; for the high mass region,  $H^\pm$  decays into top and bottom quarks. When the charged Higgs boson mass is similar to the top quark mass, the experimental signal is hard to detect because of the accompanying soft particles. For this elusive charged Higgs boson, we suggest the  $W\gamma$  decay mode as an alternative search channel. Since the branching ratio of the loop-induced decay in an ordinary two-Higgs-doublet model is very suppressed, below  $\mathcal{O}(10^{-4})$ , we extend the model by introducing a vectorlike fermion  $SU(2)$  doublet and two singlets. In type-I-II model where the SM fermions are assigned in type-I while the vectorlike fermions are in type-II, we show that the branching ratio can be greatly enhanced to  $\sim \mathcal{O}(0.01)$  in a large portion of the parameter space allowed by the Higgs precision data, the electroweak oblique parameters, and the direct search bounds at the LHC. The LHC discovery potential is also promising in the channels of  $g\bar{b} \rightarrow \bar{t}H^+(H^+ \rightarrow W^+\gamma)$  and  $gg \rightarrow H/A \rightarrow H^+W^-(H^+ \rightarrow W^+\gamma)$ .

---

## Contents

<b>1</b>	<b>Introduction</b>	<b>1</b>
<b>2</b>	<b>2HDM with Vectorlike Fermions</b>	<b>3</b>
<b>3</b>	<b>Constraints on the type-I-II 2HDM</b>	<b>6</b>
3.1	Constraints from the LHC Higgs precision data	7
3.2	Constraints from direct searches at the LHC	7
3.3	Constraints from the electroweak oblique parameter $\hat{T}$	7
3.4	Benchmark scenario for the numerical analysis	10
<b>4</b>	<b>Loop induced decays of the charged Higgs boson</b>	<b>11</b>
<b>5</b>	<b>Production of the charged Higgs boson and the LHC discovery potential for <math>H^\pm \rightarrow W^\pm \gamma</math> mode</b>	<b>15</b>
5.1	Production of the charged Higgs boson at the LHC	15
5.2	LHC discovery potential for the $H^\pm \rightarrow W^\pm \gamma$ mode	18
<b>6</b>	<b>Conclusions</b>	<b>20</b>
<b>A</b>	<b>Vacuum-polarization amplitudes of the SM gauge bosons</b>	<b>22</b>
<b>B</b>	<b>Decay Form-Factors for <math>H^\pm \rightarrow W^\pm \gamma / W^\pm Z</math></b>	<b>23</b>
B.1	Loop function	23
B.2	Decay Form-Factors from the SM quark contributions	23
B.3	Decay Form Factors from the VLQ contributions	26

---

## 1 Introduction

The current status of new physics study at the LHC is disappointing to many particle physicists as we do not see any hint for new particles. What awaits us in the near future is higher luminosity, which shall be helpful to probe some faint signals, if any, but not higher energy scale particles. Before we are resigned to the prospect of no new signal for a while, however, we must search every hole and corner. And this task requires a special strategy. The common method of finding a new particle is to resort to the main production channel and the main decay modes, which spans the bulk of the parameter space most effectively. This basic process has been performed expeditiously with dedicated

efforts, giving us various exclusion plots with a few holes and corners of the allowed region. Usually, the corners correspond to small signal rate, which will be covered as more data are coming. Problematic is the type of a blind spot or line, a very narrow allowed region, which is mainly from experimental difficulties.

A good example of the hole corresponds to the charged Higgs boson with its mass near the top-quark mass in the two-Higgs-doublet model (2HDM) [1]. Since the  $H^\pm$ - $W^\mp$ - $Z$  vertex in a 2HDM vanishes at the tree level, the charged Higgs boson mostly decays into fermions. The search strategy at the LHC [2–8] depends on its mass  $M_{H^\pm}$ . If  $M_{H^\pm} < m_t$ , the charged Higgs boson is mainly produced from the decay of a top quark in the top quark pair production, and then  $H^\pm$  decays into  $\tau\nu$ . If  $M_{H^\pm} > m_t$ , the production channel is  $g\bar{b} \rightarrow H^+\bar{t}$ , followed by the decay  $H^+ \rightarrow t\bar{b}$ . In any case, the top quark plays a key role in searching for the charged Higgs boson at the LHC, either through production or decay. Therefore, it is very difficult to probe the critical case of  $M_{H^\pm} \approx m_t$  since at least one decay product of either  $t \rightarrow H^+b$  or  $H^+ \rightarrow t\bar{b}$  is very soft [9]. We need alternative channels to target this elusive charged Higgs boson.

Non-fermionic decay channels of  $H^\pm$  into the SM particles are only the radiative decays of  $H^\pm \rightarrow W^\pm\gamma$  and  $H^\pm \rightarrow W^\pm Z$ . In the usual 2HDM, the branching ratios are very suppressed, being at most  $\sim \mathcal{O}(10^{-4})$ . So we question whether the branching ratios can be meaningfully enhanced if we extend the 2HDM by introducing vectorlike fermions (VLFs) [10]. A heavy VLF with a mass around the electroweak scale appears in many new physics models [11, 12]. One of the biggest advantages of VLFs is its consistency with the Higgs precision data unlike heavy chiral fermions [13, 14].

Increasing the branching ratios of the radiative decays, significantly enough to ensure LHC sensitivity, is very challenging. Naively raising the Yukawa couplings of the VLFs with the charged Higgs boson shall confront the constraints from the electroweak oblique parameters since the VLF loop corrections to the vertex of  $H^\pm$ - $W^\mp$ - $V$  ( $V = \gamma, Z$ ) are usually correlated with those to the vacuum polarization amplitudes of the SM gauge bosons. We need to contrive a viable model which accommodates significantly large loop-induced decays of the elusive charged Higgs boson while satisfying the other direct and indirect constraints. As will be shown, if we assign the SM fermions in type-I and the new VLFs in type-II, the goal is achieved. In a large portion of the parameter space,  $\text{Br}(H^\pm \rightarrow W^\pm\gamma)$  is greatly enhanced by one or two orders of magnitude. However, the  $WZ$  decay mode does not change much because of the strong correlation with the electroweak oblique parameter  $\hat{T}$ . This is our main result.

The  $W\gamma$  and  $WZ$  modes as a new resonance search at the LHC [15, 16] have been studied in other new physics models. A representative one is the Georgi-Machacek (GM) model [17] where the custodial-fiveplet (both singly and doubly) charged Higgs boson is fermiphobic, mainly decaying into  $WZ$  or  $WW$  through the tree level couplings [18–21]. Below the threshold of  $WZ$  or  $WW$ , the loop-induced decays into  $\gamma\gamma$ ,  $Z\gamma$ , and  $W\gamma$  were

studied [22, 23]. In a generalized inert doublet model with a broken  $Z_2$  symmetry, called the stealth Higgs doublet model,  $H^\pm \rightarrow W^\pm \gamma$  was also studied [24]. However, our model is distinguished from these models: (i) the charged Higgs boson mainly decays into fermions; (ii) the  $WZ$  decay is very suppressed, not by the kinematics, while the  $W\gamma$  decay is enhanced.

The paper is organized in the following way. In Sec. 2, we review our model, the 2HDM with the SM fermions in type-I and the VLFs in type-II. Section 3 deals with indirect and direct constraints such as the Higgs precision data, the direct searches for the charged Higgs boson and the VLFs at the LHC, and the electroweak oblique parameters. Particularly for the electroweak oblique parameter  $\hat{T}$ , we shall suggest our ansatz for the parameters. In Sec. 4, we first present the one-loop level calculation of the decay rates of  $H^\pm \rightarrow W^\pm \gamma / W^\pm Z$  via the VLF loops. This is a new calculation. Then, we show that the branching ratio of  $H^\pm \rightarrow W^\pm \gamma$  can be highly enhanced by one or two orders of magnitude, relative to that without the VLF contributions. Section 5 covers the production channels of the charged Higgs boson in our model as well as the 13 TeV LHC sensitivity to the  $H^\pm \rightarrow W^\pm \gamma$  mode. Section 6 contains our conclusions.

## 2 2HDM with Vectorlike Fermions

We consider a 2HDM with vectorlike fermions in the alignment limit. The Higgs sector is extended by introducing two complex  $SU(2)_L$  Higgs doublet scalar fields,  $\Phi_1$  and  $\Phi_2$  [1]:

$$\Phi_i = \begin{pmatrix} w_i^+ \\ \frac{v_i + h_i + i\eta_i}{\sqrt{2}} \end{pmatrix}, \quad (2.1)$$

where  $i = 1, 2$ , and  $v_{1,2}$  are the nonzero vacuum expectation values (VEVs) of  $\Phi_{1,2}$ . We parametrize  $t_\beta = v_2/v_1$  in the simplified notation of  $s_x = \sin x$ ,  $c_x = \cos x$ , and  $t_x = \tan x$ . The electroweak symmetry breaking occurs by the nonzero VEV of  $v = \sqrt{v_1^2 + v_2^2} = 246$  GeV.

The fermion sector of the SM is also extended by introducing one  $SU(2)$  doublet VLF and two  $SU(2)$  singlets as follows:

$$\begin{aligned} \text{VLF doublet : } \mathcal{Q}_L &= \begin{pmatrix} \mathcal{U}'_L \\ \mathcal{D}'_L \end{pmatrix}, \quad \mathcal{Q}_R = \begin{pmatrix} \mathcal{U}'_R \\ \mathcal{D}'_R \end{pmatrix}, \\ \text{VLF singlets : } \mathcal{U}_L, \quad \mathcal{U}_R, \quad \mathcal{D}_L, \quad \mathcal{D}_R. \end{aligned} \quad (2.2)$$

Here  $\mathcal{U}^{(l)}$  and  $\mathcal{D}^{(l)}$  denote the up-type and down-type fermions, respectively. We shall consider various kinds of the VLFs:  $(X, T)$ , the vectorlike quark (VLQ) with the electric charges of  $(5/3, 2/3)$ ;  $(T, B)$ , the VLQ with  $(2/3, -1/3)$ ;  $(B, Y)$ , the VLQ with  $(-1/3, -4/3)$ ;  $(N, E)$ , the vectorlike lepton (VLL) with  $(0, -1)$  [12].

SM	$Q_L, L_L$	$u_R$	$d_R, \ell_R$
type-I	+	-	-
VLF	$\mathcal{Q}_{L,R}$	$\mathcal{U}_{L,R}$	$\mathcal{D}_{L,R}$
type-II	+	-	+

**Table 1:** The  $Z_2$  parities of the SM fermions and VLFs.

In order to avoid the flavor changing neutral currents (FCNC) at tree level, we introduce a discrete  $Z_2$  symmetry under which  $\Phi_1 \rightarrow \Phi_1$  and  $\Phi_2 \rightarrow -\Phi_2$  [25, 26]. The  $Z_2$  parities of  $\Phi_1$  and  $\Phi_2$  dictate the scalar potential to be

$$\begin{aligned}
V_\Phi = & m_{11}^2 \Phi_1^\dagger \Phi_1 + m_{22}^2 \Phi_2^\dagger \Phi_2 - m_{12}^2 (\Phi_1^\dagger \Phi_2 + \text{H.c.}) \\
& + \frac{1}{2} \lambda_1 (\Phi_1^\dagger \Phi_1)^2 + \frac{1}{2} \lambda_2 (\Phi_2^\dagger \Phi_2)^2 + \lambda_3 (\Phi_1^\dagger \Phi_1) (\Phi_2^\dagger \Phi_2) + \lambda_4 (\Phi_1^\dagger \Phi_2) (\Phi_2^\dagger \Phi_1) \\
& + \frac{1}{2} \lambda_5 [(\Phi_1^\dagger \Phi_2)^2 + \text{h.c.}], \tag{2.3}
\end{aligned}$$

where we allow softly broken  $Z_2$  parity but maintain the  $CP$  invariance. Five physical Higgs bosons (the light  $CP$ -even scalar  $h$  at a mass of 125 GeV, the heavy  $CP$ -even scalar  $H$ , the  $CP$ -odd pseudoscalar  $A$ , and two charged Higgs bosons  $H^\pm$ ) are related with the weak eigenstates via

$$\begin{pmatrix} h_1 \\ h_2 \end{pmatrix} = \mathbb{R}(\alpha) \begin{pmatrix} H \\ h \end{pmatrix}, \quad \begin{pmatrix} \eta_1 \\ \eta_2 \end{pmatrix} = \mathbb{R}(\beta) \begin{pmatrix} z^0 \\ A \end{pmatrix}, \quad \begin{pmatrix} w_1^\pm \\ w_2^\pm \end{pmatrix} = \mathbb{R}(\beta) \begin{pmatrix} w^\pm \\ H^\pm \end{pmatrix}, \tag{2.4}$$

where  $z^0$  and  $w^\pm$  are the Goldstone bosons that will be eaten by the  $Z$  and  $W$  bosons, respectively. The rotation matrix  $\mathbb{R}(\theta)$  is

$$\mathbb{R}(\theta) = \begin{pmatrix} c_\theta & -s_\theta \\ s_\theta & c_\theta \end{pmatrix}. \tag{2.5}$$

The SM Higgs field is a linear combination of  $h$  and  $H$ ,  $h_{\text{SM}} = s_{\beta-\alpha} h + c_{\beta-\alpha} H$ . Because the observed Higgs boson at a mass of 125 GeV is very SM-like, we take the alignment limit of

$$\beta - \alpha = \frac{\pi}{2} \quad (\text{alignment limit}). \tag{2.6}$$

The fermions can have different  $Z_2$  parities. For the SM fermions, we fix  $Q_L \rightarrow Q_L$  and  $L_L \rightarrow L_L$  under  $Z_2$  parity transformation. Then, there are four different choices of  $Z_2$  parities for the right-handed SM fermion fields, leading to type-I, type-II, type-X, and type-Y. The VLFs need not to have the same  $Z_2$  parity with the SM fermions. Since our

main purpose is to explore the possibility of highly enhancing  $\text{Br}(H^\pm \rightarrow W^\pm \gamma / W^\pm Z^0)$ , we consider type-I-II, where the SM fermions are assigned in type-I while the VLFs are in type-II (see Table 1). The Lagrangian for the mass and Yukawa terms of the VLFs is then

$$-\mathcal{L}_{\text{Yuk}} = M_Q \bar{Q} Q + M_U \bar{U} U + M_D \bar{D} D + \left[ Y_{\mathcal{D}} \bar{Q} \Phi_1 \mathcal{D} + Y_U \bar{Q} \tilde{\Phi}_2 U + \text{h.c.} \right], \quad (2.7)$$

where  $\tilde{\Phi} = i\tau_2 \Phi^*$  and we take the simplified assumption of  $Y_U^L = Y_U^R \equiv Y_U$  and  $Y_{\mathcal{D}}^L = Y_{\mathcal{D}}^R \equiv Y_{\mathcal{D}}$ .

The VLF masses are from the Dirac mass parameters as well as from two VEVs of  $v_1$  and  $v_2$ . The mass matrices  $\mathbb{M}_{\mathcal{D}}$  and  $\mathbb{M}_U$  in the basis of  $(\mathcal{D}', \mathcal{D})$  and  $(U', U)$ , respectively, are

$$\mathbb{M}_{\mathcal{D}} = \begin{pmatrix} M_Q & \frac{1}{\sqrt{2}} Y_{\mathcal{D}} v c_\beta \\ \frac{1}{\sqrt{2}} Y_{\mathcal{D}} v c_\beta & M_{\mathcal{D}} \end{pmatrix}, \quad \mathbb{M}_U = \begin{pmatrix} M_Q & \frac{1}{\sqrt{2}} Y_U v s_\beta \\ \frac{1}{\sqrt{2}} Y_U v s_\beta & M_U \end{pmatrix}. \quad (2.8)$$

In the large  $t_\beta$  limit where  $c_\beta \ll 1$  and  $s_\beta \approx 1$ , the off-diagonal terms of  $\mathbb{M}_{\mathcal{D}}$  are suppressed. The VLF mass matrices are diagonalized by the rotation matrices  $\mathbb{R}(\theta_{\mathcal{F}})$  as  $\mathbb{R}(\theta_{\mathcal{F}}) \mathbb{M}_{\mathcal{F}} \mathbb{R}^T(\theta_{\mathcal{F}}) = \text{diag}(M_{\mathcal{F}_1}, M_{\mathcal{F}_2})$  for  $\mathcal{F} = U, \mathcal{D}$ . Then, the mass eigenstates of the VLFs are obtained as

$$\begin{pmatrix} \mathcal{D}_1 \\ \mathcal{D}_2 \end{pmatrix} = \mathbb{R}(\theta_{\mathcal{D}}) \begin{pmatrix} \mathcal{D}' \\ \mathcal{D} \end{pmatrix}, \quad \begin{pmatrix} U_1 \\ U_2 \end{pmatrix} = \mathbb{R}(\theta_U) \begin{pmatrix} U' \\ U \end{pmatrix}. \quad (2.9)$$

When  $\theta_{U, \mathcal{D}} \ll 1$ ,  $U_1$  and  $\mathcal{D}_1$  are  $SU(2)$  doublet-like while  $U_2$  and  $\mathcal{D}_2$  are singlet-like. In what follows, we use  $s_U = s_{\theta_U}$  and  $c_U = c_{\theta_U}$  for notational simplicity. The VLF mixing angles satisfy

$$s_{2\mathcal{D}} = \frac{\sqrt{2} Y_{\mathcal{D}} v}{M_{\mathcal{D}_2} - M_{\mathcal{D}_1}} c_\beta, \quad s_{2U} = \frac{\sqrt{2} Y_U v}{M_{U_2} - M_{U_1}} s_\beta. \quad (2.10)$$

The Yukawa Lagrangian for the SM fermions and the VLFs is

$$\begin{aligned} -\mathcal{L}_{\text{Yuk}} = & \sum_{f=t,b,\tau} \frac{m_f}{v} (\kappa_f \bar{f} f h + \xi_f^H \bar{f} f H - i \xi_f^A \bar{f} \gamma_5 f A) \\ & - \left\{ \frac{\sqrt{2}}{v} \bar{t} (m_t \xi_t^A P_L + m_b \xi_b^A P_R) b H^+ + \frac{\sqrt{2}}{v} m_\tau \xi_\ell^A \bar{\nu}_{L\tau} H^+ + \text{h.c.} \right\} \\ & + \sum_{\mathcal{F}} \sum_{i,j} \sum_{\phi} y_{\mathcal{F}_i \mathcal{F}_j}^\phi \phi \bar{\mathcal{F}}_i \mathcal{F}_j + \sum_{\mathcal{F}} \sum_{i,j} \left[ -i y_{\mathcal{F}_i \mathcal{F}_j}^A A \bar{\mathcal{F}}_{i,R} \mathcal{F}_{j,L} + \text{h.c.} \right] \\ & + \sum_{i,j} \left[ y_{U_i \mathcal{D}_j}^{H^+} H^+ \bar{U}_i \mathcal{D}_j + \text{h.c.} \right], \end{aligned} \quad (2.11)$$

where  $\mathcal{F} = U, \mathcal{D}$ ,  $i, j = 1, 2$ , and  $\phi = h, H$ . In our type-I-II model, the normalized Yukawa couplings are

$$\begin{aligned} \kappa_f = 1, \quad \xi_f^H = \frac{s_\alpha}{s_\beta}, \quad \xi_u^A = -\xi_d^A = -\xi_\ell^A = \frac{1}{t_\beta}, \\ \xi_{\mathcal{D}}^h = -s_\alpha, \quad \xi_U^h = c_\alpha, \quad \xi_{\mathcal{D}}^H = c_\alpha, \quad \xi_U^H = s_\alpha, \quad \xi_{\mathcal{D}}^A = s_\beta, \quad \xi_U^A = c_\beta. \end{aligned} \quad (2.12)$$

Additionally, we shall impose the alignment condition of  $\beta - \alpha = \pi/2$ .

The Yukawa couplings of the VLFs with neutral Higgs bosons are

$$\begin{aligned}
y_{\mathcal{F}_1\mathcal{F}_1}^\phi &= -y_{\mathcal{F}_2\mathcal{F}_2}^\phi = -\frac{1}{\sqrt{2}} Y_{\mathcal{F}} \xi_{\mathcal{F}}^\phi s_{2\mathcal{F}}, \\
y_{\mathcal{F}_1\mathcal{F}_2}^\phi &= y_{\mathcal{F}_2\mathcal{F}_1}^\phi = \frac{1}{\sqrt{2}} Y_{\mathcal{F}} \xi_{\mathcal{F}}^\phi c_{2\mathcal{F}}, \\
y_{\mathcal{F}_i\mathcal{F}_i}^A &= 0, \\
y_{\mathcal{F}_1\mathcal{F}_2}^A &= -y_{\mathcal{F}_2\mathcal{F}_1}^A = \frac{1}{\sqrt{2}} Y_{\mathcal{F}} \xi_{\mathcal{F}}^A,
\end{aligned} \tag{2.13}$$

and those with the charged Higgs boson are

$$\begin{aligned}
y_{\mathcal{U}_1\mathcal{D}_1}^{H^+} &= Y_{\mathcal{U}} \xi_{\mathcal{U}}^A c_{\mathcal{D}} s_{\mathcal{U}} + Y_{\mathcal{D}} \xi_{\mathcal{D}}^A s_{\mathcal{D}} c_{\mathcal{U}}, \\
y_{\mathcal{U}_1\mathcal{D}_2}^{H^+} &= Y_{\mathcal{U}} \xi_{\mathcal{U}}^A s_{\mathcal{D}} s_{\mathcal{U}} - Y_{\mathcal{D}} \xi_{\mathcal{D}}^A c_{\mathcal{D}} c_{\mathcal{U}}, \\
y_{\mathcal{U}_2\mathcal{D}_1}^{H^+} &= -Y_{\mathcal{U}} \xi_{\mathcal{U}}^A c_{\mathcal{D}} c_{\mathcal{U}} + Y_{\mathcal{D}} \xi_{\mathcal{D}}^A s_{\mathcal{D}} s_{\mathcal{U}}, \\
y_{\mathcal{U}_2\mathcal{D}_2}^{H^+} &= -Y_{\mathcal{U}} \xi_{\mathcal{U}}^A s_{\mathcal{D}} c_{\mathcal{U}} - Y_{\mathcal{D}} \xi_{\mathcal{D}}^A c_{\mathcal{D}} s_{\mathcal{U}}.
\end{aligned} \tag{2.14}$$

The gauge interaction Lagrangian in terms of the VLF mass eigenstates is

$$\begin{aligned}
\mathcal{L}_{\text{gauge}} &= \sum_{\mathcal{F}} \left[ e A_\mu \sum_i Q_{\mathcal{F}} \bar{\mathcal{F}}_i \gamma^\mu \mathcal{F}_i + g_Z Z_\mu \sum_{i,j} \hat{g}_{\mathcal{F}_i\mathcal{F}_j}^Z \bar{\mathcal{F}}_i \gamma^\mu \mathcal{F}_j \right] \\
&\quad + \frac{g}{\sqrt{2}} \left( \hat{g}_{\mathcal{D}_i\mathcal{U}_j}^W W_\mu^- \bar{\mathcal{D}}_i \gamma^\mu \mathcal{U}_j + \text{h.c.} \right),
\end{aligned} \tag{2.15}$$

where  $\mathcal{F} = \mathcal{U}, \mathcal{D}$ ,  $g_Z = g/c_W$ , and  $c_W$  is the cosine of the electroweak mixing angle. The normalized gauge couplings are

$$\begin{aligned}
\hat{g}_{\mathcal{F}_1\mathcal{F}_1}^Z &= g_V^{\mathcal{F}'} c_{\mathcal{F}}^2 + g_V^{\mathcal{F}} s_{\mathcal{F}}^2, & \hat{g}_{\mathcal{F}_2\mathcal{F}_2}^Z &= g_V^{\mathcal{F}'} s_{\mathcal{F}}^2 + g_V^{\mathcal{F}} c_{\mathcal{F}}^2, \\
\hat{g}_{\mathcal{F}_1\mathcal{F}_2}^Z &= \hat{g}_{\mathcal{F}_2\mathcal{F}_1}^Z = (g_V^{\mathcal{F}'} - g_V^{\mathcal{F}}) s_{\mathcal{F}} c_{\mathcal{F}}, \\
\hat{g}_{\mathcal{D}_1\mathcal{U}_1}^W &= c_{\mathcal{U}} c_{\mathcal{D}}, & \hat{g}_{\mathcal{D}_1\mathcal{U}_2}^W &= s_{\mathcal{U}} c_{\mathcal{D}}, & \hat{g}_{\mathcal{D}_2\mathcal{U}_1}^W &= c_{\mathcal{U}} s_{\mathcal{D}}, & \hat{g}_{\mathcal{D}_2\mathcal{U}_2}^W &= s_{\mathcal{U}} s_{\mathcal{D}},
\end{aligned} \tag{2.16}$$

where  $g_V^f = T_f^3 - Q_f s_W^2$ .

### 3 Constraints on the type-I-II 2HDM

Before studying how large  $\text{Br}(H^\pm \rightarrow W^\pm \gamma / W^\pm Z)$  can be, we study the allowed parameter space by the current data. First, the FCNC process of  $b \rightarrow s \gamma$  plays a sensitive probe for  $H^\pm$ . Comparing the Belle result [27] and the SM calculation with NNLO QCD correction [28–42] puts significant implications on the 2HDM [43–48]. In type-I, however, the Yukawa couplings of the charged Higgs boson with the SM fermions are all proportional to  $1/t_\beta$ . For  $t_\beta > 2$ ,  $b \rightarrow s \gamma$  does not practically constrain  $M_{H^\pm}$  [49]. Now we examine other constraints on the model such as the Higgs precision data, the direct searches for the charged Higgs boson and the VLFs at the LHC, and the electroweak oblique parameters. Based on the results, we shall suggest a benchmark scenario for this model.

### 3.1 Constraints from the LHC Higgs precision data

The new VLFs change the loop-induced  $h$ - $g$ - $g$  and  $h$ - $\gamma$ - $\gamma$  vertices which are stringently constrained by the current Higgs precision measurement. New physics effects are usually parametrized by the coupling modifier  $\kappa_i$ . Since  $\kappa_\gamma$  is mainly from  $W^\pm$  loop, the most sensitive one is  $\kappa_g$ , which the VLFs change into

$$\kappa_g = 1 + \frac{v}{A_{1/2}^H(\tau_t)} \sum_{\mathcal{F}} \sum_i \frac{y_{\mathcal{F}_i \mathcal{F}_i}^h}{M_{\mathcal{F}_i}} A_{1/2}^H(\tau_{\mathcal{F}_i}), \quad (3.1)$$

where the loop function  $A_{1/2}^H(\tau)$  is given in Ref. [72],  $\tau_f = m_h^2/m_f^2$ ,  $\mathcal{F} = \mathcal{U}, \mathcal{D}$ , and  $i = 1, 2$ . As explicitly shown in Eq. (2.13), the vectorlike nature of new fermions yields

$$y_{\mathcal{F}_1 \mathcal{F}_1}^h = -y_{\mathcal{F}_2 \mathcal{F}_2}^h. \quad (3.2)$$

Unless  $M_{\mathcal{F}_1}$  is very different from  $M_{\mathcal{F}_2}$ , the contribution from  $\mathcal{F}_1$  is considerably canceled by that from  $\mathcal{F}_2$ . The ATLAS and CMS combined result at  $2\sigma$  [73],  $0.6 < |\kappa_g| < 1.12$ , is satisfied in most of the parameter space.

### 3.2 Constraints from direct searches at the LHC

The VLQ searches have been performed by both ATLAS [50–61] and CMS [62–71] Collaborations. No signal of any VLQ gives the lower bound on the VLQ mass, depending on the assumption of the decay modes. If  $T$  ( $B$ ) decays only into  $Zt/Wb/ht$  ( $Zb/Wt/hb$ ), the bound becomes very stringent like  $M_T > 1.31$  TeV ( $M_B > 1.03$  TeV) [61]. These mass bounds are relaxed if there are other decay channels of the VLQs. For example, allowing the decay of  $T$  or  $B$  into a light quark  $q$  associated with  $W^\pm$  and  $Z$  yields  $M_Q > 690$  GeV [74]. If  $H^\pm q$  mode is additionally open, the VLQ mass bound can be weaker. As for the VLL, multi-leptonic event searches at the LHC lead to  $M_L \gtrsim 300$  GeV from the ATLAS data [75] and  $M_L \gtrsim 270$  GeV from the CMS data [76]. For the numerical analysis, therefore, we consider two cases of  $M_Q = 600$  GeV and  $M_Q = 1.3$  TeV for the VLQs, and one case of  $M_L = 300$  GeV for the VLLs.

Another important constraint from LHC direct searches is on the charged Higgs boson, the upper bound on its production cross section times branching ratio. For  $M_{H^\pm} \lesssim m_t$ , the production channel is  $pp \rightarrow tbH^\pm$  and the decay channel is  $H^\pm \rightarrow \tau\nu$ : for example,  $\sigma \cdot \text{Br} \lesssim 4$  pb when  $M_{H^\pm} = 100$  GeV at the 13 TeV LHC [77]. For  $M_{H^\pm} \gtrsim m_t$ ,  $gb \rightarrow tH^+$  ( $H^+ \rightarrow t\bar{b}$ ) is dominant. We find that the bound on  $\text{Br}(t \rightarrow bH^+) \times \text{Br}(H^\pm \rightarrow \tau^\pm\nu)$  is very efficient [77].

### 3.3 Constraints from the electroweak oblique parameter $\hat{T}$

The electroweak precision test puts one of the strongest indirect constraints on new fermions which affect the gauge boson self-energy diagrams through loops, parametrized by the

Peskin-Takeuchi oblique parameters  $S$ ,  $T$ , and  $U$  [78]. For more general parametrization, Barbieri *et al.* extended the parameters into  $\hat{S}$ ,  $\hat{T}$ ,  $W$ , and  $Y$  [79], which are defined as follows. We begin with  $\Pi_{VV'}(q^2)$ , the  $g^{\mu\nu}$  term of the transverse vacuum polarization amplitude  $\Pi_{VV'}^{\mu\nu}(q^2)$  of the gauge boson. Expanding  $\Pi_{VV'}(q^2)$  up to quadratic order as

$$\Pi_{VV'}(q^2) \simeq \Pi_{VV'}(0) + q^2 \Pi'_{VV'}(0) + \frac{(q^2)^2}{2} \Pi''_{VV'}(0) + \dots, \quad (3.3)$$

we define  $\hat{S}$ ,  $\hat{T}$ ,  $W$ , and  $Y$  as

$$\begin{aligned} \hat{S} &= \frac{g}{g'} \Pi'_{W_3 B}(0), \\ \hat{T} &= \frac{1}{m_W^2} [\Pi_{W_3 W_3}(0) - \Pi_{W^+ W^-}(0)], \\ Y &= \frac{m_W^2}{2} \Pi''_{BB}(0), \\ W &= \frac{m_W^2}{2} \Pi''_{W_3 W_3}(0). \end{aligned} \quad (3.4)$$

The traditional Peskin-Takeuchi parameters  $S$  and  $T$  are related with  $\hat{S}$  and  $\hat{T}$  as

$$S = \frac{4s_W^2}{\alpha} \hat{S}, \quad T = \frac{\hat{T}}{\alpha}. \quad (3.5)$$

The current experimental constraints are [79, 80]

$$\begin{aligned} \hat{S} &= (0.0 \pm 1.3) \times 10^{-3}, \\ \hat{T} &= (5.4 \pm 9.3) \times 10^{-4}, \\ W &= (0.1 \pm 1.2) \times 10^{-3}, \\ Y &= (-0.4 \pm 0.8) \times 10^{-3}. \end{aligned} \quad (3.6)$$

We focus on the most sensitive oblique parameter  $\hat{T}$  here.  $\hat{S}$ ,  $Y$ , and  $W$  are discussed in Appendix A. For the general vector and axial-vector gauge couplings of  $\mathcal{L} = V_\mu \bar{\psi} (g_V \gamma^\mu + g_A \gamma_5 \gamma^\mu) \psi$ ,  $\Pi_{VV'}(0)$  from a single diagram mediated by two fermions with masses  $m_a$  and  $m_b$  is [81]

$$\Pi(m_a, m_b, 0) = \frac{1}{4\pi^2} \left[ (g_V^2 + g_A^2) \tilde{\Pi}_{V+A}(m_a, m_b, 0) + (g_V^2 - g_A^2) \tilde{\Pi}_{V-A}(m_a, m_b, 0) \right], \quad (3.7)$$

where the subscript  $VV'$  in  $\Pi_{VV'}$  is omitted for simplicity and  $\tilde{\Pi}_{V\pm A}(m_a, m_b, 0)$  are

$$\begin{aligned} \tilde{\Pi}_{V+A}(m_a, m_b, 0) &= -\frac{1}{2} (m_a^2 + m_b^2) \left[ \text{Div} + \ln \left( \frac{\mu^2}{m_a m_b} \right) \right] \\ &\quad - \frac{1}{4} (m_a^2 + m_b^2) - \frac{(m_a^4 + m_b^4)}{4(m_a^2 - m_b^2)} \ln \left( \frac{m_b^2}{m_a^2} \right), \\ \tilde{\Pi}_{V-A}(m_a, m_b, 0) &= m_a m_b \left[ \text{Div} + \ln \left( \frac{\mu^2}{m_a m_b} \right) + 1 + \frac{(m_a^2 + m_b^2)}{2(m_a^2 - m_b^2)} \ln \left( \frac{m_b^2}{m_a^2} \right) \right]. \end{aligned} \quad (3.8)$$

Here  $\text{Div} = 1/\epsilon + \ln 4\pi - \gamma_\epsilon$  is the divergence term in the dimensional regularization,  $\epsilon = (4 - D)/2$ , and  $\mu$  is the renormalization scale. These divergences are properly canceled out and there is no  $\mu$  dependence on  $\hat{T}$  from the VLF contributions. The vectorlike nature of new fermions makes  $\hat{T}$  depend only on  $\tilde{\Pi}_V$ , defined by

$$\tilde{\Pi}_V = \tilde{\Pi}_{V+A} + \tilde{\Pi}_{V-A}. \quad (3.9)$$

Then,  $\hat{T}$  in our model becomes

$$\hat{T} = \frac{g^2 N_C}{16\pi^2 m_W^2} \left[ 2s_U^2 c_U^2 \tilde{\Pi}_V(M_{U_1}, M_{U_2}, 0) + 2s_D^2 c_D^2 \tilde{\Pi}_V(M_{D_1}, M_{D_2}, 0) \right. \\ \left. - 2c_U^2 c_D^2 \tilde{\Pi}_V(M_{U_1}, M_{D_1}, 0) - 2s_U^2 s_D^2 \tilde{\Pi}_V(M_{U_2}, M_{D_2}, 0) \right. \\ \left. - 2c_U^2 s_D^2 \tilde{\Pi}_V(M_{U_1}, M_{D_2}, 0) - 2s_U^2 c_D^2 \tilde{\Pi}_V(M_{U_2}, M_{D_1}, 0) \right], \quad (3.10)$$

where  $N_C = 3$  (1) for the VLQ (VLL).

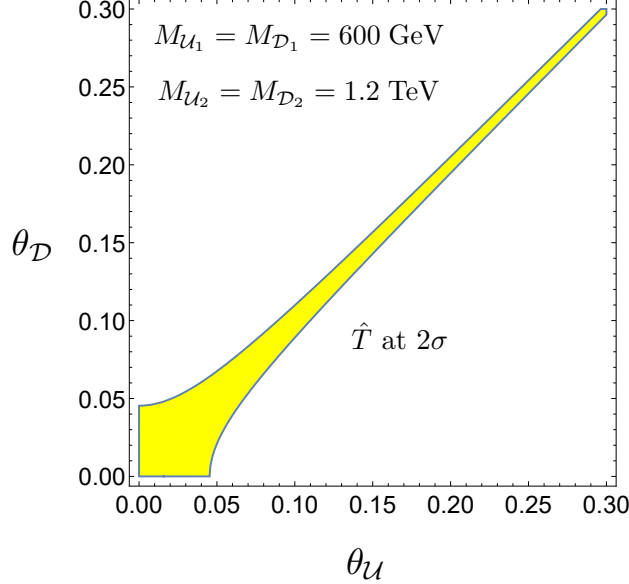


**Figure 1:** The allowed region of  $(\theta_U, \theta_D)$  at  $2\sigma$  by the electroweak oblique parameter  $\hat{T}$ . We set  $M_{U_1} = M_{D_1} = 600$  GeV and  $M_{U_2} = M_{D_2} = 1.2$  TeV.

It is generally known that the small  $\hat{T}$  prefers very degenerate masses for the new fermions in the loop, which is clearly seen from

$$\lim_{m_a \rightarrow m_b} \tilde{\Pi}_{V+A}(0) = -m_a^2 \left[ \text{Div} + \ln \left( \frac{\mu^2}{m_a^2} \right) \right] = - \lim_{m_a \rightarrow m_b} \tilde{\Pi}_{V-A}(0). \quad (3.11)$$

As will be shown, however, the crucial condition for the enhancement of  $\text{Br}(H^\pm \rightarrow W^\pm \gamma)$  is sizable mass difference between the up-type and down-type VLFs. It seems that the  $\hat{T}$  constraint excludes the possibility. Here comes the advantage of our model with *vectorlike*

$SU(2)_L$  doublet *and* singlet fermions. The new fermion spectrum includes  $\mathcal{U}_1, \mathcal{U}_2, \mathcal{D}_1$ , and  $\mathcal{D}_2$ , leading to six terms in Eq. (3.10). Now each term can be sizable while  $\hat{T}$  is kept small if the first two terms are canceled by the last four terms. We find that this cancellation occurs when  $M_{\mathcal{U}_i} \approx M_{\mathcal{D}_i}$  and  $\theta_{\mathcal{U}} \approx \theta_{\mathcal{D}}$ .

In Fig. 1, we show the  $2\sigma$  allowed region of  $(\theta_{\mathcal{U}}, \theta_{\mathcal{D}})$  by the electroweak oblique parameter  $\hat{T}$  for  $M_{\mathcal{U}_1} = M_{\mathcal{D}_1} = 600$  GeV and  $M_{\mathcal{U}_2} = M_{\mathcal{D}_2} = 1.2$  TeV. For non-negligible mixing like  $\theta_{\mathcal{U}, \mathcal{D}} \gtrsim 0.1$ ,  $\theta_{\mathcal{U}} \approx \theta_{\mathcal{D}}$  is highly required. In conclusion, we find the following simple ansatz to satisfy  $\hat{T} = 0$ :

$$M_{\mathcal{U}_1} = M_{\mathcal{D}_1}, \quad M_{\mathcal{U}_2} = M_{\mathcal{D}_2}, \quad \theta_{\mathcal{U}} = \theta_{\mathcal{D}}. \quad (3.12)$$

### 3.4 Benchmark scenario for the numerical analysis

Considering all of the constraints described above, we take the following benchmark scenario:

$$s_{\beta-\alpha} = 1, \quad (\text{alignment limit}), \quad (3.13)$$

$$M_{\mathcal{U}_1} = M_{\mathcal{D}_1} = \begin{cases} 600 \text{ GeV or } 1.3 \text{ TeV, for the VLQs;} \\ 300 \text{ GeV, for the VLLs,} \end{cases}$$

$$(Q_{\mathcal{U}}, Q_{\mathcal{D}}) = \begin{cases} \text{VLQ:} & \begin{cases} (X, T) : (5/3, 2/3); \\ (T, B) : (2/3, -1/3); \\ (B, Y) : (-1/3, -4/3); \end{cases} \\ \text{VLL:} & (N, E) : (0, -1), \end{cases}$$

$$\Delta M \equiv M_{\mathcal{U}_2} - M_{\mathcal{U}_1} = M_{\mathcal{D}_2} - M_{\mathcal{D}_1} \subset [0, 1.5] \text{ TeV},$$

$$\theta_{\mathcal{U}} = \theta_{\mathcal{D}} = 0.2,$$

where  $Q_{\mathcal{F}}$  is the electric charges of the particle  $\mathcal{F}$ . Note that the ansatz in Eq. (3.12) relates the up-type Yukawa coupling  $Y_{\mathcal{U}}$  with the down-type Yukawa coupling  $Y_{\mathcal{D}}$  as

$$Y_{\mathcal{D}} = Y_{\mathcal{U}} t_{\beta}, \quad (3.14)$$

which can be clearly seen from Eq. (2.10). For large  $t_{\beta}$ ,  $Y_{\mathcal{D}}$  becomes large.

Some brief comments on the decays of the VLQs, especially the ones with exotic electric charges in Eq. (3.13), are in order here. As being colored fermions, the VLQs are copiously produced through the pair production from the gluon fusion. The question is which Lagrangian terms determine their decay into the SM particles in our type-I-II model. For example, the  $(X, T)$  case has the following Yukawa interactions because of the  $Z_2$  parities in Table 1 and the electric charges of  $(5/3, 2/3)$ :

$$-\mathcal{L} = \delta Y_{4u} \bar{Q} \Phi_2 u_R + \delta Y_{4d} \bar{Q}_L \Phi_1 \mathcal{D} + \text{h.c.} \quad (3.15)$$

The first term leads to the mixing between  $T$  and the SM up-type quarks. The second term yields the vertices of  $X$ - $u$ - $H^{\pm}$  and  $T$ - $d$ - $H^{\pm}$ . The  $X$  decays into  $W^+ u_i$  and  $H^+ u_i$ .

## 4 Loop induced decays of the charged Higgs boson

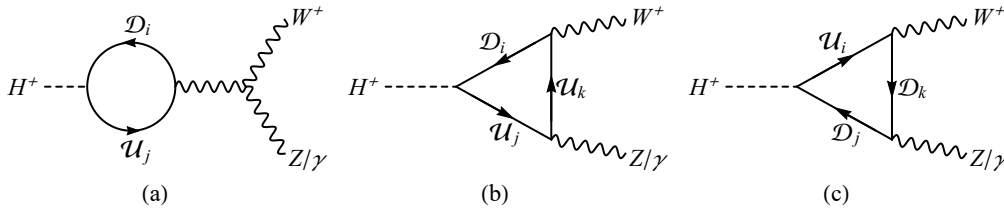


**Figure 2:** Feynman diagrams for  $H^+ \rightarrow W^+\gamma/W^+Z$ . Here  $U_i$  and  $D_i$  denote the up-type and down-type VLFs as well as the SM  $t$  and  $b$  quark, respectively.

In our model, the decays of  $H^\pm \rightarrow W^\pm\gamma$  and  $H^\pm \rightarrow W^\pm Z$  occur radiatively through the VLFs as well as the SM top and bottom quarks, as shown in Fig. 2. The loop-induced decay amplitude of  $H^+ \rightarrow W^+V$  ( $V = \gamma, Z$ ) is parametrized by

$$\mathcal{M} = \frac{g^2 N_C M_{H^\pm}}{(16\pi^2)\sqrt{2}c_W} \mathcal{M}_{\mu\nu} \varepsilon_W^{\mu*} \varepsilon_V^{\nu*}, \quad (4.1)$$

where  $N_C$  is the color factor of the fermion in the loop. We further express  $\mathcal{M}_{\mu\nu}$  in terms of three dimensionless form-factors  $\mathcal{M}_{1,2,3}$  as

$$\mathcal{M}_{\mu\nu} = g_{\mu\nu} \mathcal{M}_1 + \frac{p_{2\mu} p_{1\nu}}{M_{H^\pm}^2} \mathcal{M}_2 + i\epsilon_{\mu\nu\rho\sigma} \frac{p_{2\rho} p_{1\sigma}}{M_{H^\pm}^2} \mathcal{M}_3, \quad (4.2)$$

where  $p_1$  and  $p_2$  are the momenta of  $W^\pm$  and  $V$  respectively.

Each  $\mathcal{M}_q$  ( $q = 1, 2, 3$ ) receives the contributions from various VLF combinations through the Feynman diagrams (a), (b), and (c) in Fig. 2. Since there are two up-type VLFs and two down-type VLFs ( $\mathcal{U}_{1,2}$  and  $\mathcal{D}_{1,2}$ ), we index the form-factors by the superscripts for the diagrams and by the subscripts for the VLFs:

$$\mathcal{M}_q = \sum_{i,j} \mathcal{M}_{q,ij}^{(a)} + \sum_{i,j,k} \left[ \mathcal{M}_{q,ijk}^{(b)} + \mathcal{M}_{q,ijk}^{(c)} \right], \quad \text{for } q = 1, 2, 3. \quad (4.3)$$

We summarize the indices of  $i$ ,  $j$ , and  $k$  for  $W^\pm\gamma$  and  $W^\pm Z$  in Table 2.

	$H^+ \rightarrow W^+\gamma$	$H^+ \rightarrow W^+Z$
diagram (a): $(i, j)$	(11), (12), (21), (22)	(11), (12), (21), (22)
diagram (b) and (c): $(i, j, k)$	(111), (122), (211), (222)	(111), (112), (121), (122) (211), (212), (221), (222)

**Table 2:** The values of indices of VLQs for each diagram.

For  $W^+\gamma$  decay, the Ward-identity of  $p_2^\nu \mathcal{M}_{\mu\nu} = 0$  from the gauge invariance relates  $\mathcal{M}_1$  with  $\mathcal{M}_2$  as

$$\mathcal{M}_1 = -\frac{1}{2}(1 - \mu_W)\mathcal{M}_2, \quad \text{for } H^+ \rightarrow W^+\gamma, \quad (4.4)$$

where  $\mu_i = m_i^2/M_{H^\pm}^2$ . The partial decay rate for  $H^+ \rightarrow W^+\gamma$  is

$$\Gamma(H^+ \rightarrow W^+\gamma) = \frac{g^4 N_C^2}{2^{14} \pi^5 c_W^2} M_{H^\pm} (1 - \mu_W)^3 \left[ |\mathcal{M}_2|^2 + |\mathcal{M}_3|^2 \right]. \quad (4.5)$$

The partial decay rate for  $H^+ \rightarrow W^+Z$  is

$$\Gamma(H^+ \rightarrow W^+Z) = \frac{g^4 N_C^2 \beta}{2^{14} \pi^5 c_W^2} M_{H^\pm} \left[ \left( 6 + \frac{\beta^2}{2\mu_W \mu_Z} \right) |\mathcal{M}_1|^2 + \frac{\beta^4}{8\mu_W \mu_Z} |\mathcal{M}_2|^2 + \beta^2 |\mathcal{M}_3|^2 + \frac{\beta^2}{2} \left( \frac{1}{\mu_W \mu_Z} - \frac{1}{\mu_W} - \frac{1}{\mu_Z} \right) \text{Re}(\mathcal{M}_1 \mathcal{M}_2^*) \right], \quad (4.6)$$

where  $\beta = \sqrt{(1 - \mu_W - \mu_Z)^2 - 4\mu_W \mu_Z}$  and the Ward identity in Eq. (4.4) does not apply for the  $WZ$  mode. Note that the  $W^\pm Z$  channel is enhanced for heavy  $M_{H^\pm}$  by longitudinal polarization contribution which is proportional to  $1/(\mu_W \mu_Z)$ , i.e.,  $M_{H^\pm}^4/m_W^2 m_Z^2$ . The detailed expressions of  $\mathcal{M}_1$ ,  $\mathcal{M}_2$ , and  $\mathcal{M}_3$  from the VLF loops as well as the SM  $t$  and  $b$  quark loops [82] are shown in Appendix B. Our calculation of the VLF contributions is new. We checked that our expressions for the SM contributions are numerically consistent with those in Ref. [82].

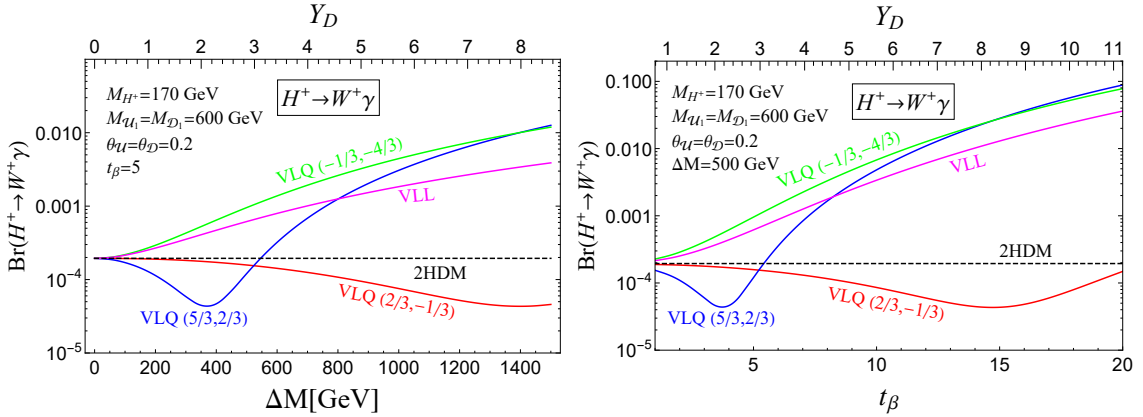


**Figure 3:**  $\text{Br}(H^+ \rightarrow W^+\gamma)$  as a function of  $\Delta M (\equiv M_{\mathcal{F}_2} - M_{\mathcal{F}_1})$  (left panel) and  $t_\beta$  (right panel). We set  $M_{\mathcal{U}_1} = M_{\mathcal{D}_1} = 600$  GeV for the VLQs,  $M_{\mathcal{U}_1} = M_{\mathcal{D}_1} = 300$  GeV for the VLLs, and  $\theta_{\mathcal{U}} = \theta_{\mathcal{D}} = 0.2$ . The numbers in the parenthesis denote the electric charges of the VLQs. The dashed lines represent the result in the type-I 2HDM without VLFs.

In Figure 3, we show the branching ratios of  $H^+ \rightarrow W^+\gamma$  as a function of  $\Delta M (\equiv M_{\mathcal{F}_2} - M_{\mathcal{F}_1})$  for the fixed  $t_\beta = 5$  (left panel), and as a function of  $t_\beta$  for the fixed  $\Delta M = 500$  GeV (right panel). We set  $M_{H^\pm} = 170$  GeV,  $M_{\mathcal{U}_1} = M_{\mathcal{D}_1} = 600$  GeV for the VLQs,

$M_{\mathcal{U}_1} = M_{\mathcal{D}_1} = 300 \text{ GeV}$  for the VLLs, and  $\theta_{\mathcal{U}} = \theta_{\mathcal{D}} = 0.2$ . Since  $Y_{\mathcal{D}} (= t_{\beta} Y_{\mathcal{U}})$  is determined by  $\Delta M$  and  $t_{\beta}$  with the given  $\theta_{\mathcal{U}}$  and  $\theta_{\mathcal{D}}$  in our ansatz, we additionally show the values of  $Y_{\mathcal{D}}$  in the plot. The value of  $Y_{\mathcal{D}}$  increases with  $\Delta M$  and  $t_{\beta}$ : too large  $\Delta M$  or  $t_{\beta}$  endangers the perturbativity of the VLF Yukawa couplings.

Let us discuss the characteristic features of  $\text{Br}(H^+ \rightarrow W\gamma)$ . First, the dashed lines are the results in the type-I 2HDM without the VLFs. The branching ratio, which is independent of  $t_{\beta}$  as a characteristic of type-I, is very suppressed like  $\sim \mathcal{O}(10^{-4})$ . It would be almost infeasible to discover the charged Higgs boson through the  $W\gamma$  decay at the LHC. When the VLFs come in the loop, the effects are not only dramatic but also very different according to their electric charges. The  $(T, B)$  case with  $(Q_{\mathcal{U}}, Q_{\mathcal{D}}) = (2/3, -1/3)$  yields smaller  $\text{Br}(H^+ \rightarrow W\gamma)$  than that without the VLFs in the whole parameter space of  $\Delta M$  and  $t_{\beta}$ : significant destructive interference with the SM contributions occurs. The  $(X, T)$  case with  $(Q_{\mathcal{U}}, Q_{\mathcal{D}}) = (5/3, 2/3)$  shows more dynamic behavior, destructive for small  $\Delta M$  or small  $t_{\beta}$  but constructive for large  $\Delta M$  or  $t_{\beta}$ . Both  $(B, Y)$  with  $(Q_{\mathcal{U}}, Q_{\mathcal{D}}) = (-1/3, -4/3)$  and  $(N, E)$  with  $(Q_{\mathcal{U}}, Q_{\mathcal{D}}) = (0, -1)$  highly enhance the branching ratio.

The whole behavior of  $\text{Br}(H^{\pm} \rightarrow W^{\pm}\gamma)$ , especially its sensitive dependence on the VLF electric charges, is not easy to understand since it involves the complicated loop effects from various combinations of the VLFs as in Fig. 2. Nevertheless, we find a reason at least when the VLF loop effects are dominant. Since  $\mathcal{M}_3(\text{VLF}) = 0$  and  $\mathcal{M}_2^{(a)} = 0$  (see Appendix B), non-vanishing contributions are from  $\mathcal{M}_2^{(b)}$  and  $\mathcal{M}_2^{(c)}$ . As can be seen in Eq. (B.14),  $\mathcal{M}_2^{(b)}$  is proportional to  $Q_{\mathcal{U}}$  while  $\mathcal{M}_2^{(c)}$  is proportional to  $Q_{\mathcal{D}}$ . In the  $(T, B)$  case, the electric charges of the up-type and down-type fermions have opposite sign, which yields substantial cancellation between  $\mathcal{M}_2^{(b)}$  and  $\mathcal{M}_2^{(c)}$ . And the remaining  $(T, B)$  contribution destructively interferes with the SM contribution. Other cases of  $(X, T)$ ,  $(B, Y)$ , and  $(N, E)$  with the same-sign electric charges for  $\mathcal{U}$  and  $\mathcal{D}$  can have large branching ratios.

Considering the direct search bound on the VLQ mass at the LHC, we show  $\text{Br}(H^+ \rightarrow W\gamma)$  for heavy VLQs with  $M_{\mathcal{U}_1} = M_{\mathcal{D}_1} = 1.31 \text{ TeV}$  in Fig. 4. Heavier VLQs with about twice mass yields much smaller  $\text{Br}(H^+ \rightarrow W\gamma)$  by an order of magnitude. But still  $\text{Br}(H^+ \rightarrow W\gamma)$  can be an order of magnitude larger than that without the VLFs.

In Figure 5, we show that the branching ratios of  $H^+ \rightarrow W^+Z$  as a function of  $\Delta M$  (left panels) and  $t_{\beta}$  (right panels). We take  $M_{H^{\pm}} = 180 \text{ GeV}$ ,  $M_{\mathcal{U}_1} = M_{\mathcal{D}_1} = 600 \text{ GeV}$  for the VLQs,  $M_{\mathcal{U}_1} = M_{\mathcal{D}_1} = 300 \text{ GeV}$  for the VLLs, and  $\theta_{\mathcal{U}} = \theta_{\mathcal{D}} = 0.2$ . The VLQ loop contribution to  $H^{\pm} \rightarrow W^{\pm}Z$  is not as large as that to  $H^{\pm} \rightarrow W^{\pm}\gamma$ , typically a few tens of percent for  $Y_{\mathcal{D}} \simeq 5$ . We find that there is a strong correlation between  $\text{Br}(H^{\pm} \rightarrow W^{\pm}Z)$  and the constraint from the electroweak oblique parameter  $\hat{T}$ .

The reader may question whether the large enhancement of  $\text{Br}(H^{\pm} \rightarrow W^{\pm}\gamma)$  happens only in the benchmark scenario. To answer the question, we scan all of the

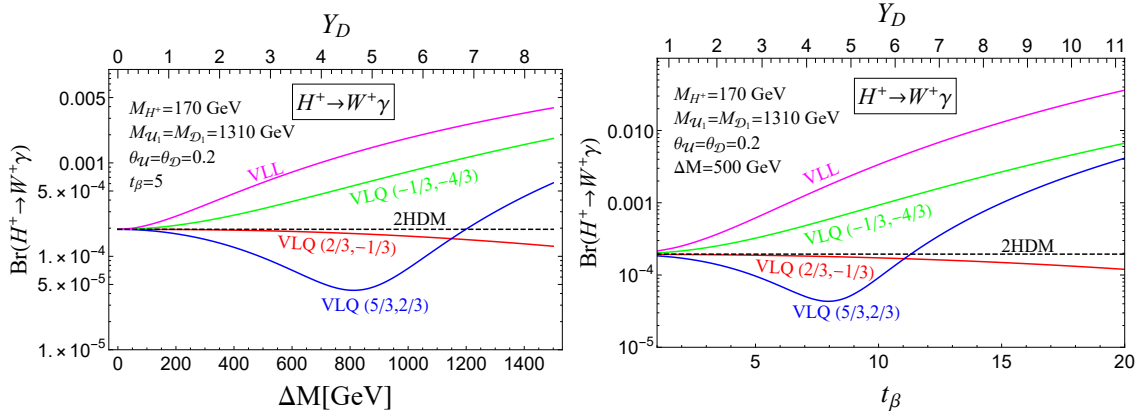


**Figure 4:**  $\text{Br}(H^+ \rightarrow W\gamma)$  with heavy VLFs in the loop as a function of  $\Delta M$  (left panels) and  $t_\beta$  (right panels). We set  $M_{U_1} = M_{D_2} = 1.31 \text{ TeV}$  for the VLQs,  $M_{U_1} = M_{D_1} = 300 \text{ GeV}$  for the VLLs, and  $\theta_U = \theta_D = 0.2$ . The dashed lines represent the result of the type-I 2HDM without VLFs.

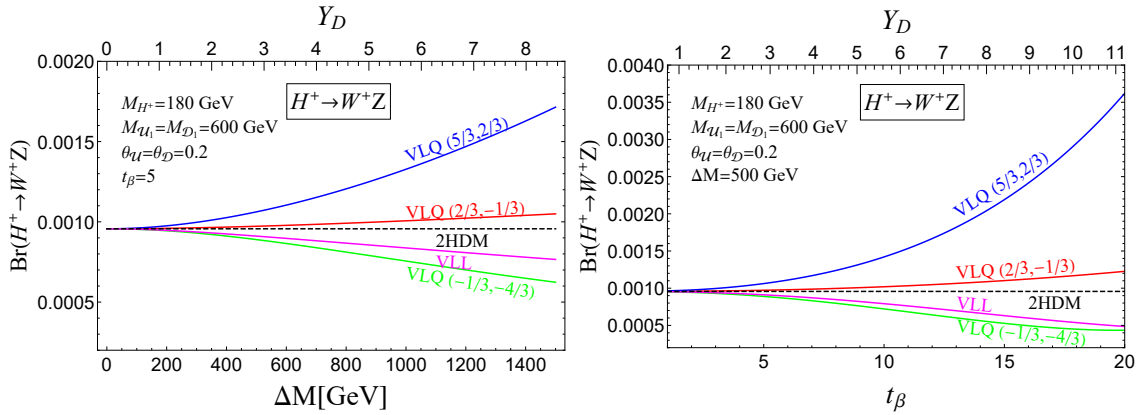


**Figure 5:**  $\text{Br}(H^+ \rightarrow W^+Z)$  as a function of  $\Delta M$  (left panels) and  $t_\beta$  (right panels). We set  $M_{U_1} = M_{D_1} = 600 \text{ GeV}$  for the VLQs,  $M_{U_1} = M_{D_1} = 300 \text{ GeV}$  for the VLLs, and  $\theta_U = \theta_D = 0.2$ . The numbers in the parenthesis denote the electric charges of VLQ. The dashed lines represent the result in type-I 2HDM without the VLFs.

parameters in the range of

$$\begin{aligned}
 M_{\mathcal{F}_1} < M_{\mathcal{F}_2} &\in [600, 3000] \text{ GeV} \quad (\text{for the VLQ with low mass}), & (4.7) \\
 M_{\mathcal{F}_1} < M_{\mathcal{F}_2} &\in [1310, 5000] \text{ GeV} \quad (\text{for the VLQ with high mass}), \\
 M_{\mathcal{F}_1} < M_{\mathcal{F}_2} &\in [300, 1500] \text{ GeV} \quad (\text{for the VLL}), \\
 t_\beta &\in [1, 50], \quad \theta_U, \theta_D \in \left[-\frac{\pi}{2}, \frac{\pi}{2}\right].
 \end{aligned}$$

Note that we independently span  $\theta_U$  and  $\theta_D$ , not imposing the condition of  $\theta_U = \theta_D$ .  $Y_U$  and  $Y_D$  are determined by Eq. (2.10). Then we select the parameter sets that satisfy the constraints from the Higgs precision data on  $\kappa_g$ , the upper bound on

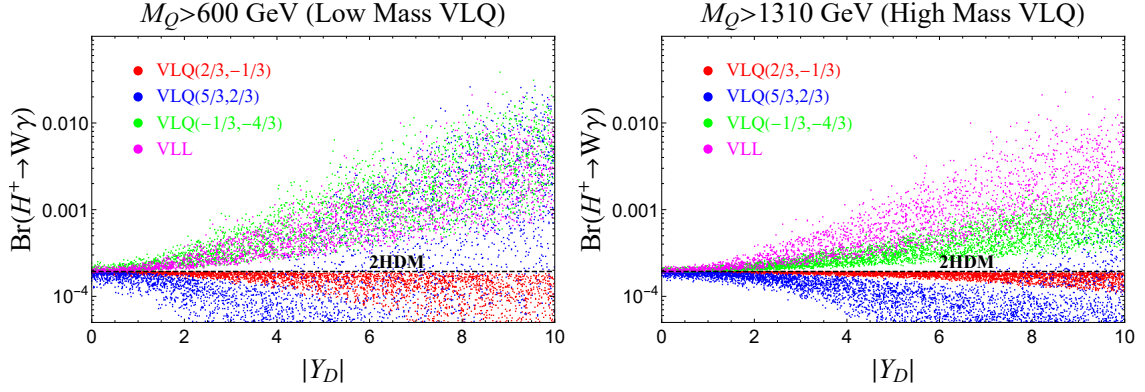


**Figure 6:** Scatter plots for  $\text{Br}(H^+ \rightarrow W\gamma)$  from the parameter sets which satisfy all of the experimental constraints. Dashed lines represent the results of the 2HDM without the VLFs.

$\text{Br}(t \rightarrow bH^\pm) \times \text{Br}(H^\pm \rightarrow \tau^\pm\nu)$ , the electroweak oblique parameter  $\hat{T}$ , and the perturbativity  $|Y_{U,D}| < 4\pi$ . For the surviving parameter sets, we show the scatter plots of  $\text{Br}(H^+ \rightarrow W\gamma)$  as a function of  $|Y_D|$  for the VLQs with low masses (left panel) and with high masses (right panel) in Fig. 6. It is true that the benchmark scenario in Eq. (3.13) yields very enhanced  $\text{Br}(H^\pm \rightarrow W^\pm\gamma)$ , though not the maximum. Nonetheless, considerable parameter sets for the  $(X, T)$ ,  $(B, Y)$ , and  $(N, E)$  cases allow at least one order of magnitude enhancement of  $\text{Br}(H^\pm \rightarrow W^\pm\gamma)$  for  $|Y_D| \gtrsim 5$ . It is fair to say that the VLFs in our model greatly enhance the branching ratio of  $H^\pm \rightarrow W^\pm\gamma$ . Concerning the details, the benchmark point for the  $(X, T)$  case does not represent the whole parameter space: even for large  $|Y_D| \gtrsim 5$ , the  $(X, T)$  contribution to  $\text{Br}(H^\pm \rightarrow W^\pm\gamma)$  can be very destructive or very constructive, while the benchmark point always enhances the branching ratio. For heavier VLQ masses (right panel), the range of the scatter plot is not as wide as that for low VLQ masses. The scatter ranges of the  $(X, T)$ ,  $(T, B)$ , and  $(B, Y)$  cases are quite separated.

## 5 Production of the charged Higgs boson and the LHC discovery potential for $H^\pm \rightarrow W^\pm\gamma$ mode

### 5.1 Production of the charged Higgs boson at the LHC

At the LHC, the charged Higgs boson in a 2HDM is produced in two ways, through the SM particles or through the resonant decay of  $H$  or  $A$ . The first category includes

$$\begin{aligned}
 gg &\rightarrow t\bar{t}(t \rightarrow bH^+), \quad gg \rightarrow \bar{t}bH^+, \\
 g\bar{b} &\rightarrow \bar{t}H^+, \\
 q\bar{q} &\rightarrow H^+H^-.
 \end{aligned}
 \tag{5.1}$$

Other production processes such as  $q\bar{q}' \rightarrow H^+h/H^+H$ ,  $c\bar{s} \rightarrow H^+$  and  $b\bar{b} \rightarrow W^-H^+$  have very small cross section, one order of magnitude smaller than those in Eq. (5.1).

Note that all of these production processes occur at tree level: the VLFs do not play a role here.

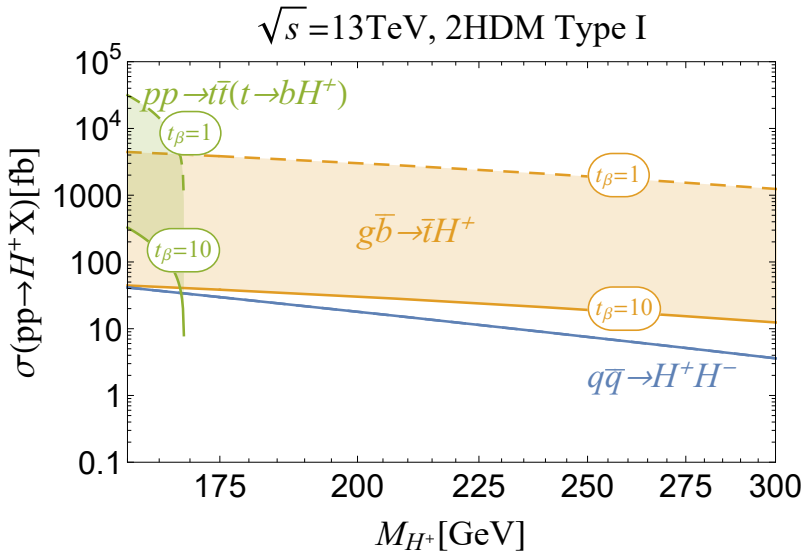


**Figure 7:** Production cross sections of the charged Higgs boson as a function of its mass at the 13 TeV LHC. We consider two cases of  $t_\beta = 1$  (dashed line) and  $t_\beta = 10$  (solid line).

In Fig. 7, we show the cross sections of the production channels in Eq. (5.1) as a function of  $M_{H^\pm}$  at the LHC with  $\sqrt{s} = 13 \text{ TeV}$ . We consider two cases,  $t_\beta = 1$  (dashed line) and  $t_\beta = 10$  (solid line). We use NNPDF [83] for the parton distribution function inside the proton. For  $M_{H^\pm} \lesssim m_t$ , the dominant production channel is from  $t\bar{t}$  production, followed by  $t \rightarrow H^+ b$ . The result is based on the calculation of  $\sigma(pp \rightarrow t\bar{t}) \times \text{Br}(t \rightarrow H^+ b)$  where we use the next-to-next-to-leading order result of  $\sigma_{t\bar{t}} = 831.8_{-29}^{+20} \pm 35 \text{ pb}$  with a top quark mass  $m_t = 172.5 \text{ GeV}$  at the 13 TeV LHC [84]. The cross section quickly falls down by kinematics as  $M_{H^\pm}$  approaches to  $m_t$ . The  $t_\beta$  dependence on  $\sigma(gg \rightarrow tbH^+)$  is very large. The cross section with  $t_\beta = 1$  is about 100 times that with  $t_\beta = 10$ , which is attributed to the  $t$ - $b$ - $H^+$  vertex being proportional to  $1/t_\beta$ . Note that the  $t_\beta$  dependence on the production cross section is opposite to that on  $\text{Br}(H^\pm \rightarrow W^\pm \gamma)$ .

For  $M_{H^\pm} \gtrsim m_t$ , the production process of  $g\bar{b} \rightarrow \bar{t}H^+$  becomes dominant. The LO analytic expression for the production process can be found in Ref. [85]. The higher order QCD corrections are given in Ref. [86–88]. In this work, we only use the LO result. The  $t_\beta$  dependence on  $\sigma(g\bar{b} \rightarrow \bar{t}H^+)$  is the same as that on  $\sigma(gg \rightarrow tbH^+)$ : small  $t_\beta$  yields much larger production cross section. The pair production  $q\bar{q} \rightarrow H^+ H^-$  is via  $s$ -channel diagrams mediated by  $\gamma$  and  $Z$ , which is independent of  $t_\beta$ . We adopt the LO analytic result in Ref. [89]. The production cross section is very small in the whole range of  $M_{H^\pm}$ , being  $\mathcal{O}(1) \sim \mathcal{O}(10) \text{ fb}$ .

Another way to produce the charged Higgs boson at the LHC is through the resonant decay of other heavy Higgs bosons. The heavy neutral Higgs bosons,  $H$

and  $A$ , are produced through the gluon fusion, followed by their decay into a charged Higgs boson:

$$gg \rightarrow H/A \rightarrow H^\pm W^\mp, \quad gg \rightarrow H \rightarrow H^+ H^-. \quad (5.2)$$

Note that the gluon fusion production of  $H$  or  $A$  is not significantly affected by the VLFs: (i) the scattering amplitudes of  $gg \rightarrow A$  are proportional to the axial-vector coupling of the fermion in the loop, which vanishes for the VLFs; (ii) for  $gg \rightarrow H$ , to which only the  $H\mathcal{F}_1\mathcal{F}_1$  and  $H\mathcal{F}_2\mathcal{F}_2$  ( $\mathcal{F} = \mathcal{U}, \mathcal{D}$ ) vertices contribute, the relation of  $y_{\mathcal{F}_1\mathcal{F}_1}^H = -y_{\mathcal{F}_2\mathcal{F}_2}^H$  yields considerable cancellation of the VLQ contributions. For the resonant decay of  $H$  or  $A$ , we make use of the  $W^\pm$  boson as a well-defined tagging particle, in order to reduce the model dependence. Then the decays of  $H \rightarrow H^\pm W^\mp$  and  $A \rightarrow H^\pm W^\mp$  go through the following Lagrangian terms:

$$\mathcal{L} \supset i \frac{e}{2s_W} W_\mu^- \left[ s_{\beta-\alpha} \left( H^+ \partial^\mu H - H \partial^\mu H^+ \right) - i \left( H^+ \partial^\mu A - A \partial^\mu H^+ \right) \right]. \quad (5.3)$$

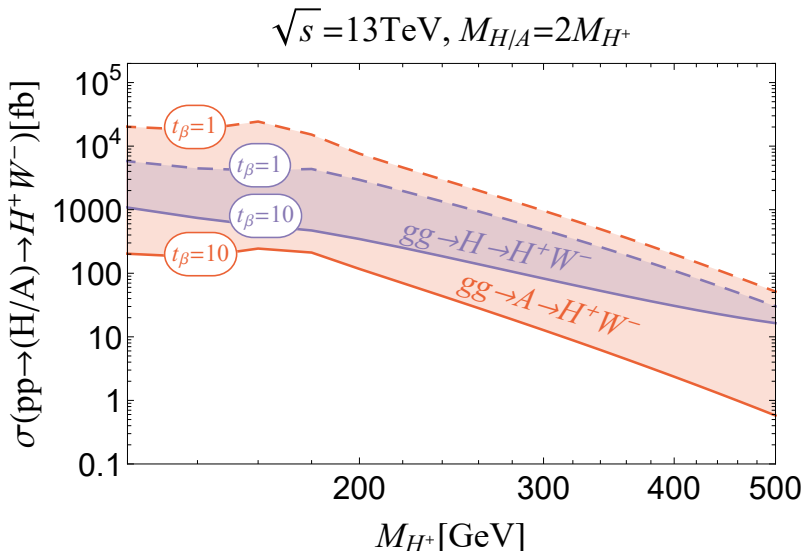


**Figure 8:** Cross sections of the resonance production channels for the charged Higgs boson at the LHC as a function of its mass. We use the HIGLU Fortran package [90] for estimating NNLO K-factors for neutral Higgs production. We set  $M_{\mathcal{U}_1} = M_{\mathcal{D}_1} = 600$  GeV,  $M_{\mathcal{U}_2} = M_{\mathcal{D}_2} = 1200$  GeV,  $\theta_{\mathcal{U}} = \theta_{\mathcal{D}} = 0.2$ , and  $M_{H/A} = 2M_{H^\pm}$ . We consider two cases of  $t_\beta = 1$  (dashed line) and  $t_\beta = 10$  (solid line).

Figure 8 shows the production cross section of  $gg \rightarrow H/A \rightarrow H^\pm W^\mp$  as a function of  $M_{H^\pm}$ . We set  $M_{H/A} = 2M_{H^\pm}$ ,  $M_{\mathcal{U}_1} = M_{\mathcal{D}_1} = 600$  GeV,  $\Delta M = 600$  GeV, and  $\theta_{\mathcal{U}} = \theta_{\mathcal{D}} = 0.2$  for two cases of  $t_\beta = 1$  (dashed line) and  $t_\beta = 10$  (solid line). Both  $gg \rightarrow H \rightarrow H^\pm W^\mp$  and  $gg \rightarrow A \rightarrow H^\pm W^\mp$  have sizable cross section of  $\mathcal{O}(1) \sim \mathcal{O}(10)$  pb when  $M_{H^\pm} = m_t$ . For  $t_\beta = 1$ ,  $gg \rightarrow A \rightarrow H^\pm W^\mp$  is more dominant while for large  $t_\beta$ ,  $gg \rightarrow H \rightarrow H^\pm W^\mp$  is more important. A crucial factor is the

unknown parameter  $M_{H/A}$ , which is set to be  $2M_{H^\pm}$  in Fig. 8. For larger  $M_{H/A}$ ,  $\sigma(gg \rightarrow H/A)$  drops very steeply: if we set  $M_{H/A} = 500$  GeV,  $\sigma(gg \rightarrow H)$  is about 30% of that with  $M_H = 2M_{H^\pm}$  and  $\sigma(gg \rightarrow A)$  is only 10%.  $\text{Br}(H/A \rightarrow H^+W^-)$  decreases only a few percent.

## 5.2 LHC discovery potential for the $H^\pm \rightarrow W^\pm\gamma$ mode

Next, we consider the potential for the LHC to observe the elusive charged Higgs boson with  $M_{H^\pm} \simeq m_t$  through the  $W\gamma$  channel. We ask whether the  $5\sigma$  discovery is possible with the total integrated luminosity  $300 \text{ fb}^{-1}$ . The answer largely depends on its production channel. In the previous section, we have studied three production channels, through the top quark pair production of  $gg \rightarrow t\bar{t}(t \rightarrow H^+b)$ , the single top quark production of  $g\bar{b} \rightarrow H^+\bar{t}$ , and the heavy Higgs boson production of  $gg \rightarrow H/A \rightarrow H^+W^-$ . When  $M_{H^\pm} \simeq m_t$ , two processes of  $gg \rightarrow t\bar{t}(t \rightarrow H^+b)$  and  $g\bar{b} \rightarrow H^+\bar{t}$  have similar production cross sections of  $\mathcal{O}(10) \sim \mathcal{O}(10^3)$  fb, depending on the value of  $t_\beta$  (see Fig. 7). However, the process  $gg \rightarrow \bar{t}H^+b(H^+ \rightarrow W^+\gamma)$  has the final states  $\bar{t}W^+b\gamma$ : the irreducible background is the top quark pair production accompanied with a photon. As a top-quark factory, it shall be very difficult for the LHC to detect  $H^\pm \rightarrow W^\pm\gamma$  via the  $gg \rightarrow t\bar{t}$  channel. Therefore, we focus on two production channels of  $g\bar{b} \rightarrow H^+\bar{t}$  and  $gg \rightarrow H/A \rightarrow H^+W^-$ . In order to suppress the SM background, we require the invariant mass of  $W^\pm$  and  $\gamma$  to be<sup>1</sup>

$$|M_{W+\gamma}| < (170 \pm 10) \text{ GeV}. \quad (5.4)$$

First, the  $g\bar{b} \rightarrow H^+\bar{t}$  process, followed by  $H^+ \rightarrow W^+\gamma$ , has the irreducible background of the single top quark production with a  $W$  boson and a photon<sup>2</sup>. The SM cross section of the  $tW$  production at NNLO is  $\sigma = 71.7 \pm 1.8(\text{scale}) \pm 3.4(\text{PDF})$  pb [91], which is an order of magnitude smaller than the  $t\bar{t}$  production. Under the additional cut in Eq. (5.4), the SM result for  $\sigma(pp \rightarrow \bar{t}W^+\gamma)$  at  $\sqrt{s} = 13$  TeV is about 5.5 fb by using MadGraph [92]. With a total integrated luminosity of  $300 \text{ fb}^{-1}$ , the  $5\sigma$  discovery through both  $pp \rightarrow \bar{t}W^+\gamma$  and  $pp \rightarrow tW^-\gamma$  channels demands the new signal more than about 0.48 fb, based on the significance of  $S/\sqrt{B}$  without including the systematic uncertainties.

In Fig. 9, we show  $\sigma(g\bar{b} \rightarrow \bar{t}H^+) \times \text{Br}(H^+ \rightarrow W^+\gamma)$  as a function of  $t_\beta$  at the 13 TeV LHC. We set  $M_{H^\pm} = 170$  GeV,  $M_{\mathcal{U}_1} = M_{\mathcal{D}_1} = 600$  GeV for the VLQs,  $M_{\mathcal{U}_1} = M_{\mathcal{D}_1} = 300$  GeV for the VLLs, and  $\Delta M = 600$  GeV. The opposite  $t_\beta$  dependences on  $\sigma(g\bar{b} \rightarrow \bar{t}H^+)$  and  $\text{Br}(H^+ \rightarrow W^+\gamma)$  lead to rather gentle increase of  $\sigma \times \text{Br}$  about  $t_\beta$ , except for the  $(X, T)$  case with  $t_\beta \lesssim 7$ . The most promising case is  $(B, Y)$ , which has  $\sigma \times \text{Br} \gtrsim 0.2$  fb. The parameter region with  $t_\beta \gtrsim 10.5$  can be probed with  $5\sigma$  significance. For the  $(X, T)$  case,  $t_\beta \gtrsim 11$  can be discovered at  $5\sigma$ . Neither the  $(T, B)$  nor  $(N, E)$  case can be probed in the whole range of  $t_\beta$ .

<sup>1</sup> More optimized kinematic cuts can enhance the significance, which is beyond the scope of this paper.

<sup>2</sup> The  $tW$  production was first observed by the ATLAS and CMS Collaborations using 7 TeV data [93, 94] as well as at the 13 TeV [95, 96], but the  $tW\gamma$  production process has not been discovered yet.

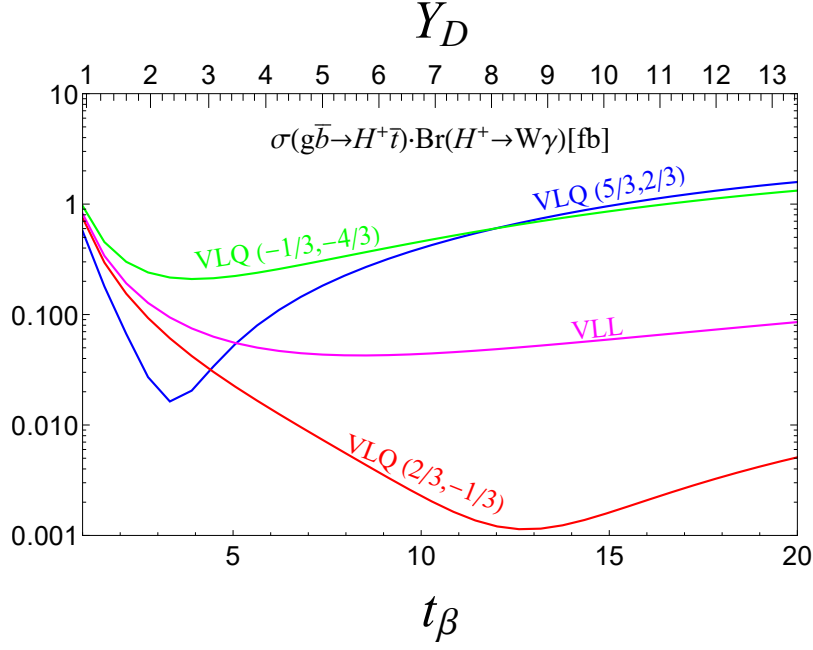


**Figure 9:**  $\sigma(g\bar{b} \rightarrow \bar{t}H^+) \times \text{Br}(H^+ \rightarrow W^+\gamma)$  as a function of  $t_\beta$  at the 13 TeV LHC. We set  $M_{H^\pm} = 170$  GeV,  $M_{\mathcal{U}_1} = M_{\mathcal{D}_1} = 600$  GeV, and  $\Delta M = 600$  GeV.

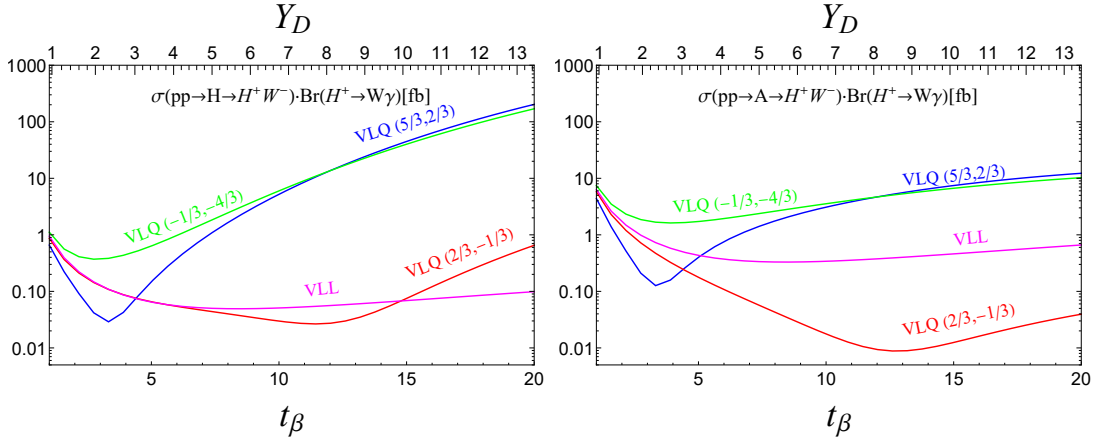


**Figure 10:**  $\sigma(gg \rightarrow H/A \rightarrow H^+W^-) \times \text{Br}(H^+ \rightarrow W^+\gamma)$  as a function of  $t_\beta$  at the 13 TeV LHC. We set  $M_{H^\pm} = 170$  GeV,  $M_H = M_A = 2M_{H^\pm}$ ,  $M_{\mathcal{U}_1} = M_{\mathcal{D}_1} = 600$  GeV for the VLQs,  $M_{\mathcal{U}_1} = M_{\mathcal{D}_1} = 300$  GeV for the VLLs, and  $\Delta M = 600$  GeV.

Next we present  $\sigma(gg \rightarrow H/A \rightarrow H^+W^-) \times \text{Br}(H^+ \rightarrow W^+\gamma)$  as a function of  $t_\beta$  in Fig. 10, the  $H$  mediated one (left panel) and the  $A$  mediated one (right panel). We set  $M_{H^\pm} = 170$  GeV,  $M_H = M_A = 2M_{H^\pm}$ ,  $M_{\mathcal{U}_1} = M_{\mathcal{D}_1} = 600$  GeV for the VLQs,  $M_{\mathcal{U}_1} = M_{\mathcal{D}_1} = 300$  GeV for the VLLs, and  $\Delta M = 600$  GeV. Since the suppression of the production cross section by large  $t_\beta$  is weak for the  $H$  mediation as shown in Fig. 8, the increase of  $\sigma \times \text{Br}$  with respect to  $t_\beta$  is much larger for the

$gg \rightarrow H$  production channel. With the kinematic cut in Eq. (5.4), the SM result for  $\sigma(pp \rightarrow W^+W^-\gamma)$  at  $\sqrt{s} = 13$  TeV is about 14.4 fb by using MadGraph. Including both  $H^+W^-$  and  $H^-W^+$ , the  $5\sigma$  discovery with the total integrated luminosity of  $300 \text{ fb}^{-1}$  requires  $\sigma \times \text{Br} \gtrsim 0.77$  fb. Through the  $H$  resonance channel, the  $(B, Y)$  and  $(X, T)$  cases can be probed for  $t_\beta \gtrsim 5.2$  and  $t_\beta \gtrsim 6.9$  at  $5\sigma$ , respectively. Neither the  $(T, B)$  nor  $(N, E)$  case has a chance to be detected at the LHC. For the  $gg \rightarrow A$  production channel, we can see the  $(B, Y)$  case in the whole range of  $t_\beta$ , and the  $(X, T)$  case for  $t_\beta \gtrsim 6$ . And both  $(N, E)$  and  $(T, B)$  cases for small  $t_\beta \lesssim 3$  can be also probed.

Although the significance increases if we include both  $H$  and  $A$  channels, it would be insignificant without knowing the masses of  $H$  and  $A$ . If  $M_H = M_A = 500$  GeV, for example, the production cross section of  $H$  ( $A$ ) becomes only 30% (10%) of that with  $M_{H/A} = 2M_{H^\pm}$ . Then, through the  $gg \rightarrow H$  channel, the  $(B, Y)$  and  $(X, T)$  case can be probed at  $5\sigma$  for  $t_\beta \gtrsim 8.2$  and  $t_\beta \gtrsim 8.8$ , respectively. In the  $A$  resonance channel, only very large  $t_\beta$  region can be probed: the  $(X, T)$  case with  $t_\beta \gtrsim 15.5$  and the  $(B, Y)$  case with  $t_\beta \gtrsim 16.7$ .

## 6 Conclusions

Targeting the elusive charged Higgs boson  $H^\pm$  with its mass similar to the top-quark mass, we have explored the theoretical possibility that its radiative decays into  $W^\pm\gamma$  and  $W^\pm Z$  are large enough to detect  $H^\pm$  at the LHC. We considered a two-Higgs-doublet model with a vectorlike fermion (VLF)  $SU(2)$  doublet  $\mathcal{Q}$  and two singlets  $\mathcal{U}$  and  $\mathcal{D}$ . Various VLF cases with different electric charges have been studied, including the vectorlike lepton  $(N, E)$  with the electric charge  $(0, -1)$  as well as the vectorlike quarks  $(X, T)$  with  $(5/3, 2/3)$ ,  $(T, B)$  with  $(2/3, -1/3)$ , and  $(B, Y)$  with  $(-1/3, -4/3)$ . For the large enhancement of the loop-induced decays, we suggest the type-I-II 2HDM where the SM fermions are assigned in type-I while the VLFs are in type-II.

Introducing a VLF doublet and two singlets, necessary for the interaction with the Higgs doublet fields, plays a crucial role. As being vectorlike, one generation of the new fermions has two up-type fermions,  $\mathcal{U}_1$  and  $\mathcal{U}_2$ , and two down-type fermions,  $\mathcal{D}_1$  and  $\mathcal{D}_2$ . And these extended fermions allow significant cancellation among the different VLF contributions to the Higgs precision data as well as to the electroweak oblique parameters, especially  $\hat{T}$ . Sizable cancellation to the  $h$ - $g$ - $g$  vertex occurs naturally because the  $h\mathcal{F}_1\mathcal{F}_1$  coupling is opposite to  $h\mathcal{F}_2\mathcal{F}_2$ . The cancellation for the electroweak oblique parameter  $\hat{T}$  requires some fine-tuning. We proposed an ansatz to ensure  $\hat{T} = 0$  such that  $M_{\mathcal{U}_1} = M_{\mathcal{D}_1}$ ,  $M_{\mathcal{U}_2} = M_{\mathcal{D}_2}$ , and  $\theta_{\mathcal{U}} = \theta_{\mathcal{D}}$ , which is not so artificial. We have also included the constraints from direct search bounds on the VLFs and the charged Higgs boson at the LHC.

We presented the loop-induced amplitudes of  $H^\pm \rightarrow W^\pm\gamma$  and  $H^\pm \rightarrow W^\pm Z$  from the VLFs as well as the SM  $t$  and  $b$  quarks. For the  $(B, Y)$  and  $(N, E)$  cases,

$\text{Br}(H^\pm \rightarrow W^\pm\gamma)$  is shown to be enhanced in the whole parameter region, particularly for large  $\Delta M(= M_{U_2} - M_{U_1})$  and large  $t_\beta$ : if  $\Delta M \simeq 500 \text{ GeV}$  and  $t_\beta = 10$ , the enhancement is by two orders of magnitude. For the  $(X, T)$  case, the behavior of  $\text{Br}(H^\pm \rightarrow W^\pm\gamma)$  is dynamic: for small  $\Delta M$  or small  $t_\beta$ , destructive interference with the SM contributions occurs; for large  $\Delta M$  or  $t_\beta$ , the  $(X, T)$  contribution becomes dominant, greatly enhancing the branching ratio. The  $(T, B)$  case always yields a smaller signal rate than in the 2HDM without the VLFs, because the opposite signs of the electric charges of  $T$  and  $B$  bring about sizable cancellation among new fermion contributions and the remaining VLF contribution destructively interferes with the SM contributions. On the contrary,  $\text{Br}(H^\pm \rightarrow W^\pm Z)$  is very moderately affected by the VLFs, because of the strong correlation with the electroweak oblique parameter  $\hat{T}$ . Therefore, we focused on the  $W\gamma$  mode to probe the elusive charged Higgs boson at the LHC.

We have also studied the production of the charged Higgs boson. At the LHC, the main production is through the top quark (a single or pair production) or through the resonant decay of a heavy Higgs boson  $H$  or  $A$ . Since the  $t\bar{t}$  production, followed by  $t \rightarrow H^+b$  and  $H^+ \rightarrow W^+\gamma$ , has too large SM background of  $pp \rightarrow t\bar{b}W^+\gamma$ , we considered two processes,  $g\bar{b} \rightarrow tH^+$  and  $gg \rightarrow H/A \rightarrow H^+W^-$ . Based on the parton level calculation at the 13 TeV LHC with the total integrated luminosity  $300 \text{ fb}^{-1}$ , we showed that the charged Higgs boson via  $W\gamma$  mode can be probed at  $5\sigma$  in some cases. Through the  $g\bar{b} \rightarrow tH^+$  production, both the  $(X, T)$  and  $(B, Y)$  cases have the  $5\sigma$  level potential if  $\Delta M \gtrsim 500 \text{ GeV}$  and  $t_\beta \gtrsim 10$ . Neither the  $(T, B)$  nor  $(N, E)$  case has enough significance for the discovery. The prospect of the  $gg \rightarrow H/A \rightarrow H^\pm W^\mp$  channel sensitively depends on the masses of heavy Higgs bosons,  $H$  and  $A$ . If their masses are in the desirable range, e.g.,  $M_{H/A} \simeq 2M_{H^\pm}$ , this channel can also probe the  $H^\pm \rightarrow W^\pm\gamma$  mode for the  $(X, T)$  and  $(B, Y)$  cases with  $\Delta M \gtrsim 500 \text{ GeV}$  and  $t_\beta \gtrsim 5$ .

In conclusion, the radiative decay mode  $W\gamma$  can serve as an alternative channel to probe the elusive charged Higgs boson. A theoretically viable model in the extended type-I 2HDM with the vectorlike fermions was suggested to allow the great enhancement of the  $W\gamma$  branching ratio. We expect that this study helps the LHC to search for the charged Higgs boson.

## Acknowledgments

We thank Eung Jin Chun for the helpful comments. The work of J.S. was supported by the National Research Foundation of Korea, Grant No. NRF-2016R1D1A1B03932102. Y.W.Y was supported by Basic Science Research Program through the National Research Foundation of Korea, Grant No. 2017R1A6A3A11036365.

## A Vacuum-polarization amplitudes of the SM gauge bosons

For the electroweak oblique parameters  $\hat{S}$ ,  $Y$ , and  $W$ , we need the first and second derivatives of the transverse vacuum polarization amplitudes of the SM gauge bosons, which are explicitly shown in Ref. [81]. However, we found some typos in their results. The correct ones are

$$\begin{aligned} \tilde{\Pi}'_{V+A}(0) = & \frac{1}{3} \left[ \text{Div} + \ln \left( \frac{\mu^2}{m_a m_b} \right) \right] + \frac{m_a^4 - 8m_a^2 m_b^2 + m_b^4}{9(m_a^2 - m_b^2)^2} \\ & + \frac{(m_a^2 + m_b^2)(m_a^4 - 4m_a^2 m_b^2 + m_b^4)}{6(m_a^2 - m_b^2)^3} \ln \left( \frac{m_b^2}{m_a^2} \right), \end{aligned} \quad (\text{A.1})$$

$$\tilde{\Pi}'_{V-A}(0) = m_a m_b \left[ \frac{(m_a^2 + m_b^2)}{2(m_a^2 - m_b^2)^2} + \frac{m_a^2 m_b^2}{(m_a^2 - m_b^2)^3} \ln \left( \frac{m_b^2}{m_a^2} \right) \right], \quad (\text{A.2})$$

$$\tilde{\Pi}''_{V+A}(0) = \frac{(m_a^2 + m_b^2)(m_a^4 - 8m_a^2 m_b^2 + m_b^4)}{4(m_a^2 - m_b^2)^4} - \frac{3m_a^4 m_b^4}{(m_a^2 - m_b^2)^5} \ln \left( \frac{m_b^2}{m_a^2} \right), \quad (\text{A.3})$$

$$\tilde{\Pi}''_{V-A}(0) = m_a m_b \left[ \frac{(m_a^4 + 10m_a^2 m_b^2 + m_b^4)}{3(m_a^2 - m_b^2)^4} + \frac{2(m_a^2 + m_b^2)m_a^2 m_b^2}{(m_a^2 - m_b^2)^5} \ln \left( \frac{m_b^2}{m_a^2} \right) \right]. \quad (\text{A.4})$$

In our type-I-II 2HDM,  $\hat{S}$  is

$$\begin{aligned} \hat{S} = & \frac{g^2 N_C}{16\pi^2 m_W^2} \left[ c_U^2 (2Q_U - c_U^2) \tilde{\Pi}'_V(M_{U_1}, M_{U_1}, 0) + s_U^2 (2Q_U - s_U^2) \tilde{\Pi}'_V(M_{U_2}, M_{U_2}, 0) \right. \\ & - c_D^2 (2Q_D + c_D^2) \tilde{\Pi}'_V(M_{D_1}, M_{D_1}, 0) - s_D^2 (2Q_D + s_D^2) \tilde{\Pi}'_V(M_{D_2}, M_{D_2}, 0) \\ & \left. - 2s_U^2 c_U^2 \tilde{\Pi}'_V(M_{U_1}, M_{U_2}, 0) - 2s_D^2 c_D^2 \tilde{\Pi}'_V(M_{D_1}, M_{D_2}, 0) \right], \end{aligned} \quad (\text{A.5})$$

where  $N_C = 3$  (1) for VLQ (VLL) is the color factor.  $Y$  and  $W$  are

$$\begin{aligned} W = & \frac{g^2 m_W^2 N_C}{32\pi^2} \left[ c_U^4 \tilde{\Pi}''_V(M_{U_1}, M_{U_1}, 0) + s_U^4 \tilde{\Pi}''_V(M_{U_2}, M_{U_2}, 0) \right. \\ & + c_D^4 \tilde{\Pi}''_V(M_{D_1}, M_{D_1}, 0) + s_D^4 \tilde{\Pi}''_V(M_{D_2}, M_{D_2}, 0) \\ & \left. + 2s_U^2 c_U^2 \tilde{\Pi}''_V(M_{U_1}, M_{U_2}, 0) + 2s_D^2 c_D^2 \tilde{\Pi}''_V(M_{D_1}, M_{D_2}, 0) \right], \end{aligned} \quad (\text{A.6})$$

$$Y = \left( \frac{g'}{g} \right)^2 W. \quad (\text{A.7})$$

## B Decay Form-Factors for $H^\pm \rightarrow W^\pm \gamma / W^\pm Z$

### B.1 Loop function

For the one loop calculation, we express the result in term of the loop functions of the LoopTools [97]. Two point function defines  $B_i$ 's as

$$B_0(p^2, m_1^2, m_2^2) \equiv \frac{\mu^{4-D}}{i\pi^{D/2}r_\Gamma} \int d^D q \frac{1}{[q^2 - m_1^2] [(q+p)^2 - m_2^2]}, \quad (\text{B.1})$$

$$p_\mu B_1(p^2, m_1^2, m_2^2) \equiv \frac{\mu^{4-D}}{i\pi^{D/2}r_\Gamma} \int d^D q \frac{q_\mu}{[q^2 - m_1^2] [(q+p)^2 - m_2^2]}, \quad (\text{B.2})$$

where  $\mu$  is the renormalization scale,  $D = 4 - 2\epsilon$ , and  $r_\Gamma = \Gamma^2(1 - \epsilon)\Gamma(1 + \epsilon)/\Gamma(1 - 2\epsilon)$ .

The tensorial integral for the one-loop three point function is defined by

$$T_{\mu_1 \dots \mu_P}^3(p_1^2, p_2^2, (p_1 + p_2)^2, m_1^2, m_2^2, m_3^2) \equiv \frac{\mu^{4-D}}{i\pi^{D/2}r_\Gamma} \int d^D q \frac{q_{\mu_1} \dots q_{\mu_P}}{[q^2 - m_1^2] [(q+p_1)^2 - m_2^2] [(q+p_1+p_2)^2 - m_3^2]}. \quad (\text{B.3})$$

The decompositions of the tensorial integrals up to rank 2 are

$$\begin{aligned} T^3 &= C_0, \\ T_\mu^3 &= k_{1\mu} C_1 + k_{2\mu} C_2, \\ T_{\mu\nu}^3 &= g_{\mu\nu} C_{00} + \sum_{i,j=1}^2 k_{i\mu} k_{j\nu} C_{ij}, \end{aligned} \quad (\text{B.4})$$

where  $k_1 = p_1$  and  $k_2 = p_1 + p_2$ . All of the coefficient functions of  $B_i$ ,  $C_i$  and  $C_{ij}$  are numerically computed by LoopTools. Note that  $C_{00}$  and  $B_i$  have UV divergence which should be canceled out.

### B.2 Decay Form-Factors from the SM quark contributions

We describe the form factors defined in Eq. (4.2) for each single diagram shown in Figure 2. We compute the diagrams in the unitary gauge, and use the dimensional regularization with  $D = 4 - 2\epsilon$  in the  $\overline{\text{MS}}$  scheme. As for the UV divergence, we show only the  $1/\epsilon$  term. Since there is no tree-level coupling for the  $H^+ W^- V$  vertex, all of the UV divergences should be canceled out among themselves after summing all the diagrams. This cancellation serves as a validation of the calculation. For notational simplicity, we introduce the normalized gauge couplings and Yukawa couplings as

$$\begin{aligned} \hat{g}_{ff}^\gamma &= s_W c_W Q_f, & \hat{g}_{WW}^Z &= c_W^2, & \hat{g}_{WW}^\gamma &= -s_W c_W, \\ \hat{g}_{Zff}^L &= T_f^3 - Q_f s_W^2, & \hat{g}_{Zff}^R &= -Q_f s_W^2 \\ y_{H^+tb}^L &= \frac{\sqrt{2} V_{tb} m_t}{vt_\beta}, & y_{H^+tb}^R &= -\frac{\sqrt{2} V_{tb} m_b}{vt_\beta}. \end{aligned} \quad (\text{B.5})$$

We first present the results for  $H^+ \rightarrow W^+\gamma$ . In the SM model, the main contribution is from the top and bottom quarks. Since the decay involves a photon,  $\mathcal{M}_1$  is determined by  $\mathcal{M}_2$  through the Ward identity in Eq. (4.4). We separately present the expressions of  $\mathcal{M}_2$  and  $\mathcal{M}_3$  from the diagrams (a), (b), and (c) in Fig. 2.  $\mathcal{M}_2$ 's are

$$\mathcal{M}_2^{(a)} = 0, \tag{B.6}$$

$$\mathcal{M}_2^{(b)} = 2\hat{g}_{tt}^\gamma M_{H^\pm} \left[ y_{H^+tb}^L m_t (C_1 - C_2 - 2C_{12} - 2C_{22}) - y_{H^+tb}^R m_b (C_0 + C_1 + 3C_2 + 2C_{12} + 2C_{22}) \right],$$

$$\mathcal{M}_2^{(c)} = \mathcal{M}_2^{(b)} \left( y_{H^+tb}^L \leftrightarrow y_{H^+tb}^R, t \leftrightarrow b \right), \tag{B.7}$$

and  $\mathcal{M}_3$ 's are

$$\mathcal{M}_3^{(a)} = 0, \tag{B.8}$$

$$\mathcal{M}_3^{(b)} = 2\hat{g}_{tt}^\gamma M_{H^\pm} \left[ y_{H^+tb}^R m_b (C_0 + C_1 + C_2) + y_{H^+tb}^L m_t (C_1 + C_2) \right],$$

$$\mathcal{M}_3^{(c)} = -\mathcal{M}_3^{(b)} \left( y_{H^+tb}^L \leftrightarrow y_{H^+tb}^R, t \leftrightarrow b \right). \tag{B.9}$$

Here  $C_l$  and  $C_{lm}$  are

$$C_{l,lm} = C_{l,lm}(m_W^2, 0, M_{H^+}^2, m_b^2, m_t^2, m_t^2). \tag{B.10}$$

For  $H^+ \rightarrow W^+Z$ ,  $\mathcal{M}_1$  is not related with  $\mathcal{M}_2$ , given by

$$\begin{aligned}
\mathcal{M}_1^{(a)} &= -\frac{\hat{g}_{WW}^Z}{M_{H^\pm}} \left(1 - \frac{m_Z^2}{m_W^2}\right) \left[ y_{H^+tb}^R m_b \left( B_0 + B_1 + \frac{1}{\epsilon} \right) + y_{H^+tb}^L m_t \left( B_1 - \frac{1}{\epsilon} \right) \right], \quad (\text{B.11}) \\
\mathcal{M}_1^{(b)} &= \frac{y_{H^+tb}^R m_b}{M_{H^+}} \left[ \hat{g}_{Ztt}^L m_W^2 \left( C_0 + 3C_1 + C_2 + 2C_{11} + 2C_{12} \right) \right. \\
&\quad - \hat{g}_{Ztt}^L m_Z^2 \left( C_0 + C_1 + C_2 + 2C_{12} \right) \\
&\quad - \hat{g}_{Ztt}^L \left\{ 1 - 4C_{00} - M_{H^+}^2 (C_0 + C_1 + 3C_2 + 2C_{12} + 2C_{22}) \right\} \\
&\quad \left. - 2\hat{g}_{Ztt}^R m_t^2 C_0 + \frac{\hat{g}_{Ztt}^L}{\epsilon} \right] \\
&\quad + \frac{y_{H^+tb}^L m_t}{M_{H^+}} \left[ \hat{g}_{Ztt}^L m_W^2 \left( 2C_1 + C_2 + 2C_{11} + 2C_{12} \right) - \hat{g}_{Ztt}^R m_W^2 \left( C_1 + 2C_{11} + 2C_{12} \right) \right. \\
&\quad - \hat{g}_{Ztt}^L m_Z^2 \left( C_2 + 2C_{12} \right) + \hat{g}_{Ztt}^R m_Z^2 \left( C_1 + 2C_{12} \right) \\
&\quad - \hat{g}_{Ztt}^L \left\{ 1 - 4C_{00} - M_{H^+}^2 (C_2 + 2C_{12} + 2C_{22}) \right\} \\
&\quad + \hat{g}_{Ztt}^R \left\{ 1 - 8C_{00} - M_{H^+}^2 (C_1 + 2C_2 + 2C_{12} + 2C_{22}) \right\} \\
&\quad \left. + \frac{(\hat{g}_{Ztt}^L - 2\hat{g}_{Ztt}^R)}{\epsilon} \right], \\
\mathcal{M}_1^{(c)} &= \mathcal{M}_1^{(b)} \left( y_{H^+tb}^L \leftrightarrow y_{H^+tb}^R, t \leftrightarrow b \right).
\end{aligned}$$

The  $\mathcal{M}_2$  and  $\mathcal{M}_3$  for  $H^\pm \rightarrow W^\pm Z$  are

$$\begin{aligned}
\mathcal{M}_2^{(a)} &= 0, \quad (\text{B.12}) \\
\mathcal{M}_2^{(b)} &= -2y_{H^+tb}^R m_b M_{H^\pm} \hat{g}_{Ztt}^L (C_0 + C_1 + 3C_2 + 2C_{12} + 2C_{22}) \\
&\quad + 2y_{H^+tb}^L m_t M_{H^\pm} \left[ -\hat{g}_{Ztt}^L (C_2 + 2C_{12} + 2C_{22}) + \hat{g}_{Ztt}^R C_1 \right], \\
\mathcal{M}_2^{(c)} &= \mathcal{M}_2^{(b)} \left( y_{H^+tb}^L \leftrightarrow y_{H^+tb}^R, t \leftrightarrow b \right), \\
\mathcal{M}_3^{(a)} &= 0, \\
\mathcal{M}_3^{(b)} &= 2y_{H^+tb}^R m_b M_{H^\pm} \hat{g}_{Ztt}^L (C_0 + C_1 + C_2) + 2y_{H^+tb}^L m_t M_{H^\pm} (\hat{g}_{Ztt}^L C_2 + \hat{g}_{Ztt}^R C_1), \\
\mathcal{M}_3^{(c)} &= -\mathcal{M}_3^{(b)} \left( y_{H^+tb}^L \leftrightarrow y_{H^+tb}^R, t \leftrightarrow b \right).
\end{aligned}$$

The  $B_l$  and  $C_{lm}$  are as follows:

$$\begin{aligned}
B_l &= B_l(M_{H^+}^2, m_b^2, m_t^2), \\
C_{lm} &= C_{lm}(m_W^2, m_Z^2, M_{H^+}^2, m_b^2, m_t^2, m_t^2). \quad (\text{B.13})
\end{aligned}$$

### B.3 Decay Form Factors from the VLQ contributions

We first present the form factors of  $\mathcal{M}_2$  and  $\mathcal{M}_3$  for  $H^\pm \rightarrow W^\pm V$  ( $V = \gamma, Z$ ) through the VLQ loop as

$$\begin{aligned}
\mathcal{M}_{2,ij}^{(a)} &= 0, \\
\mathcal{M}_{2,ijk}^{(b)} &= 4\hat{g}_{\mathcal{D}_i\mathcal{U}_k}^W \hat{g}_{\mathcal{U}_k\mathcal{U}_j}^V y_{\mathcal{U}_j\mathcal{D}_i}^{H^+} M_{H^\pm} \\
&\quad \times \left[ M_{\mathcal{U}_k} C_1 - M_{\mathcal{D}_i} (C_0 + C_1 + 3C_2 + 2C_{12} + 2C_{22}) \right. \\
&\quad \left. - M_{\mathcal{U}_j} (C_2 + 2C_{12} + 2C_{22}) \right], \\
\mathcal{M}_{2,ijk}^{(c)} &= 4\hat{g}_{\mathcal{D}_k\mathcal{U}_i}^W \hat{g}_{\mathcal{D}_j\mathcal{D}_k}^V y_{\mathcal{U}_i\mathcal{D}_j}^{H^+} M_{H^\pm} \left[ \mathcal{U} \leftrightarrow \mathcal{D} \right], \\
\mathcal{M}_{3,ij}^{(a)} &= \mathcal{M}_{3,ijk}^{(b)} = \mathcal{M}_{3,ijk}^{(c)} = 0,
\end{aligned} \tag{B.14}$$

where  $[\mathcal{U} \leftrightarrow \mathcal{D}]$  denotes interchanging  $\mathcal{U}$  and  $\mathcal{D}$  for the terms in the square parenthesis of the previous formula while remaining the indices. Note that  $\mathcal{M}_{3,ijk}^{(b)} = \mathcal{M}_{3,ijk}^{(c)} = 0$  because of the vectorlike nature of the VLFs, i.e.,  $y_{H^+\mathcal{U}\mathcal{D}}^L = y_{H^+\mathcal{U}\mathcal{D}}^R$ . The full expressions of  $B_l$ ,  $C_l$ , and  $C_{lm}$  are

$$\begin{aligned}
B_l &= B_l(M_{H^\pm}^2, M_{\mathcal{D}_i}^2, M_{\mathcal{U}_j}^2), \\
C_{l,lm} &= C_{l,lm}(m_W^2, m_V^2, M_{H^\pm}^2, M_{\mathcal{D}_i}^2, M_{\mathcal{U}_k}^2, M_{\mathcal{U}_j}^2).
\end{aligned} \tag{B.16}$$

For  $H^\pm \rightarrow W^\pm Z$ ,  $\mathcal{M}_1$ 's are independent from  $\mathcal{M}_2$ , given by

$$\mathcal{M}_{1,ij}^{(a)} = 2\hat{g}_{\mathcal{D}_i\mathcal{U}_j}^W \hat{g}_{WW}^Z y_{\mathcal{U}_j\mathcal{D}_i}^{H^\pm} \frac{1}{M_{H^\pm}} \left( 1 - \frac{m_Z^2}{m_W^2} \right) \times \left[ -2M_{\mathcal{D}_i} B_0 - 2(M_{\mathcal{D}_i} + M_{\mathcal{U}_j}) B_1 + \frac{1}{\epsilon} (M_{\mathcal{U}_j} - M_{\mathcal{D}_i}) \right], \quad (\text{B.17})$$

$$\mathcal{M}_{1,ijk}^{(b)} = 2\hat{g}_{\mathcal{D}_i\mathcal{U}_k}^W \hat{g}_{\mathcal{U}_k\mathcal{U}_j}^Z y_{\mathcal{U}_j\mathcal{D}_i}^{H^\pm} \frac{1}{M_{H^\pm}} \times \left[ M_{\mathcal{D}_i} m_W^2 (C_0 + 3C_1 + C_2 + 2C_{11} + 2C_{12}) - M_{\mathcal{D}_i} m_Z^2 (C_0 + C_1 + C_2 + 2C_{12}) \right. \\ \left. + M_{\mathcal{D}_j} m_W^2 (2C_1 + C_2 + 2C_{11} + 2C_{12}) - M_{\mathcal{D}_j} m_Z^2 (C_2 + 2C_{12}) \right. \\ \left. - M_{\mathcal{D}_k} m_W^2 (C_1 + 2C_{11} + 2C_{12}) + M_{\mathcal{D}_k} m_Z^2 (C_1 + 2C_{12}) \right. \\ \left. - M_{\mathcal{D}_i} \{ 1 - 4C_{00} - M_{H^\pm}^2 (C_0 + C_1 + 3C_2 + 2C_{12} + 2C_{22}) \} \right. \\ \left. - M_{\mathcal{U}_j} \{ 1 - 4C_{00} - M_{H^\pm}^2 (C_2 + 2C_{12} + 2C_{22}) \} \right. \\ \left. + M_{\mathcal{U}_k} \{ 1 - 8C_{00} - M_{H^\pm}^2 (C_1 + 2C_2 + 2C_{12} + 2C_{22}) \} \right. \\ \left. - 2M_{\mathcal{D}_i} M_{\mathcal{U}_j} M_{\mathcal{U}_k} C_0 + \frac{1}{\epsilon} (M_{\mathcal{D}_i} + M_{\mathcal{U}_j} - 2M_{\mathcal{U}_k}) \right], \quad (\text{B.18})$$

$$\mathcal{M}_{1,ijk}^{(c)} = 2\hat{g}_{\mathcal{D}_k\mathcal{U}_i}^W \hat{g}_{\mathcal{D}_j\mathcal{D}_k}^Z y_{\mathcal{U}_i\mathcal{D}_j}^{H^\pm} \frac{1}{M_{H^\pm}} \left[ \mathcal{U} \leftrightarrow \mathcal{D} \right].$$

## References

- [1] G. C. Branco, P. M. Ferreira, L. Lavoura, M. N. Rebelo, M. Sher and J. P. Silva, Phys. Rept. **516**, 1 (2012) doi:10.1016/j.physrep.2012.02.002 [arXiv:1106.0034 [hep-ph]].
- [2] G. Aad *et al.* [ATLAS Collaboration], JHEP **1503**, 088 (2015) doi:10.1007/JHEP03(2015)088 [arXiv:1412.6663 [hep-ex]].
- [3] V. Khachatryan *et al.* [CMS Collaboration], JHEP **1511**, 018 (2015) doi:10.1007/JHEP11(2015)018 [arXiv:1508.07774 [hep-ex]].
- [4] G. Aad *et al.* [ATLAS Collaboration], Eur. Phys. J. C **73**, no. 6, 2465 (2013) doi:10.1140/epjc/s10052-013-2465-z [arXiv:1302.3694 [hep-ex]].
- [5] V. Khachatryan *et al.* [CMS Collaboration], JHEP **1512**, 178 (2015) doi:10.1007/JHEP12(2015)178 [arXiv:1510.04252 [hep-ex]].
- [6] A. M. Sirunyan *et al.* [CMS Collaboration], JHEP **1811**, 115 (2018) doi:10.1007/JHEP11(2018)115 [arXiv:1808.06575 [hep-ex]].
- [7] M. Aaboud *et al.* [ATLAS Collaboration], Phys. Lett. B **759**, 555 (2016) doi:10.1016/j.physletb.2016.06.017 [arXiv:1603.09203 [hep-ex]].
- [8] G. Aad *et al.* [ATLAS Collaboration], JHEP **1603**, 127 (2016) doi:10.1007/JHEP03(2016)127 [arXiv:1512.03704 [hep-ex]].
- [9] M. Aaboud *et al.* [ATLAS Collaboration], JHEP **1811**, 085 (2018) doi:10.1007/JHEP11(2018)085 [arXiv:1808.03599 [hep-ex]].

- [10] J. Ellis, S. A. R. Ellis, J. Quevillon, V. Sanz and T. You, *JHEP* **1603**, 176 (2016) doi:10.1007/JHEP03(2016)176 [arXiv:1512.05327 [hep-ph]].
- [11] L. Lavoura and J. P. Silva, *Phys. Rev. D* **47**, 2046 (1993). doi:10.1103/PhysRevD.47.2046
- [12] J. A. Aguilar-Saavedra, R. Benbrik, S. Heinemeyer and M. Prez-Victoria, *Phys. Rev. D* **88**, no. 9, 094010 (2013) doi:10.1103/PhysRevD.88.094010 [arXiv:1306.0572 [hep-ph]].
- [13] C. Anastasiou, S. Buehler, E. Furlan, F. Herzog and A. Lazopoulos, *Phys. Lett. B* **702**, 224 (2011) doi:10.1016/j.physletb.2011.06.097 [arXiv:1103.3645 [hep-ph]].
- [14] C. Anastasiou, C. Duhr, F. Dulat, E. Furlan, T. Gehrmann, F. Herzog, A. Lazopoulos and B. Mistlberger, *JHEP* **1605**, 058 (2016) doi:10.1007/JHEP05(2016)058 [arXiv:1602.00695 [hep-ph]].
- [15] G. Aad *et al.* [ATLAS Collaboration], *Phys. Lett. B* **738**, 428 (2014) doi:10.1016/j.physletb.2014.10.002 [arXiv:1407.8150 [hep-ex]].
- [16] M. Aaboud *et al.* [ATLAS Collaboration], *Phys. Rev. D* **98**, no. 3, 032015 (2018) doi:10.1103/PhysRevD.98.032015 [arXiv:1805.01908 [hep-ex]].
- [17] H. Georgi and M. Machacek, *Nucl. Phys. B* **262**, 463 (1985). doi:10.1016/0550-3213(85)90325-6
- [18] C. W. Chiang and K. Yagyu, *JHEP* **1301**, 026 (2013) doi:10.1007/JHEP01(2013)026 [arXiv:1211.2658 [hep-ph]].
- [19] C. W. Chiang, G. Cottin and O. Eberhardt, *Phys. Rev. D* **99**, no. 1, 015001 (2019) doi:10.1103/PhysRevD.99.015001 [arXiv:1807.10660 [hep-ph]].
- [20] K. Hartling, K. Kumar and H. E. Logan, *Phys. Rev. D* **90**, no. 1, 015007 (2014) doi:10.1103/PhysRevD.90.015007 [arXiv:1404.2640 [hep-ph]].
- [21] C. W. Chiang, S. Kanemura and K. Yagyu, *Phys. Rev. D* **90**, no. 11, 115025 (2014) doi:10.1103/PhysRevD.90.115025 [arXiv:1407.5053 [hep-ph]].
- [22] H. E. Logan and Y. Wu, *JHEP* **1811**, 121 (2018) doi:10.1007/JHEP11(2018)121 [arXiv:1809.09127 [hep-ph]].
- [23] C. Degrande, K. Hartling and H. E. Logan, *Phys. Rev. D* **96**, no. 7, 075013 (2017) Erratum: [*Phys. Rev. D* **98**, no. 1, 019901 (2018)] doi:10.1103/PhysRevD.96.075013, 10.1103/PhysRevD.98.019901 [arXiv:1708.08753 [hep-ph]].
- [24] R. Enberg, J. Rathsman and G. Wouda, *Phys. Rev. D* **91**, no. 9, 095002 (2015) doi:10.1103/PhysRevD.91.095002 [arXiv:1311.4367 [hep-ph]].
- [25] S. L. Glashow and S. Weinberg, *Phys. Rev. D* **15**, 1958 (1977). doi:10.1103/PhysRevD.15.1958
- [26] E. A. Paschos, *Phys. Rev. D* **15**, 1966 (1977). doi:10.1103/PhysRevD.15.1966
- [27] T. Saito *et al.* [Belle Collaboration], *Phys. Rev. D* **91**, no. 5, 052004 (2015) doi:10.1103/PhysRevD.91.052004 [arXiv:1411.7198 [hep-ex]].
- [28] K. G. Chetyrkin, M. Misiak and M. Munz, *Phys. Lett. B* **400**, 206 (1997) Erratum: [*Phys. Lett. B* **425**, 414 (1998)] doi:10.1016/S0370-2693(97)00324-9 [hep-ph/9612313].
- [29] A. J. Buras, A. Kwiatkowski and N. Pott, *Phys. Lett. B* **414**, 157 (1997) Erratum: [*Phys. Lett. B* **434**, 459 (1998)] doi:10.1016/S0370-2693(98)00853-3, 10.1016/S0370-2693(97)01142-8 [hep-ph/9707482].

- [30] A. J. Buras, A. Czarnecki, M. Misiak and J. Urban, Nucl. Phys. B **631**, 219 (2002) doi:10.1016/S0550-3213(02)00261-4 [hep-ph/0203135].
- [31] M. Misiak and M. Steinhauser, Nucl. Phys. B **683**, 277 (2004) doi:10.1016/j.nuclphysb.2004.02.006 [hep-ph/0401041].
- [32] M. Neubert, Eur. Phys. J. C **40**, 165 (2005) doi:10.1140/epjc/s2005-02141-1 [hep-ph/0408179].
- [33] K. Melnikov and A. Mitov, Phys. Lett. B **620**, 69 (2005) doi:10.1016/j.physletb.2005.06.015 [hep-ph/0505097].
- [34] M. Misiak *et al.*, Phys. Rev. Lett. **98**, 022002 (2007) doi:10.1103/PhysRevLett.98.022002 [hep-ph/0609232].
- [35] M. Misiak and M. Steinhauser, Nucl. Phys. B **764**, 62 (2007) doi:10.1016/j.nuclphysb.2006.11.027 [hep-ph/0609241].
- [36] M. Czakon, U. Haisch and M. Misiak, JHEP **0703**, 008 (2007) doi:10.1088/1126-6708/2007/03/008 [hep-ph/0612329].
- [37] R. Boughezal, M. Czakon and T. Schutzmeier, JHEP **0709**, 072 (2007) doi:10.1088/1126-6708/2007/09/072 [arXiv:0707.3090 [hep-ph]].
- [38] T. Ewerth, Phys. Lett. B **669**, 167 (2008) doi:10.1016/j.physletb.2008.09.045 [arXiv:0805.3911 [hep-ph]].
- [39] M. Misiak and M. Steinhauser, Nucl. Phys. B **840**, 271 (2010) doi:10.1016/j.nuclphysb.2010.07.009 [arXiv:1005.1173 [hep-ph]].
- [40] A. Ferroglia and U. Haisch, Phys. Rev. D **82**, 094012 (2010) doi:10.1103/PhysRevD.82.094012 [arXiv:1009.2144 [hep-ph]].
- [41] M. Misiak and M. Poradzinski, Phys. Rev. D **83**, 014024 (2011) doi:10.1103/PhysRevD.83.014024 [arXiv:1009.5685 [hep-ph]].
- [42] M. Czakon, P. Fiedler, T. Huber, M. Misiak, T. Schutzmeier and M. Steinhauser, JHEP **1504**, 168 (2015) doi:10.1007/JHEP04(2015)168 [arXiv:1503.01791 [hep-ph]].
- [43] P. Ciafaloni, A. Romanino and A. Strumia, Nucl. Phys. B **524**, 361 (1998) doi:10.1016/S0550-3213(98)00190-4 [hep-ph/9710312].
- [44] M. Ciuchini, G. Degrossi, P. Gambino and G. F. Giudice, Nucl. Phys. B **527**, 21 (1998) doi:10.1016/S0550-3213(98)00244-2 [hep-ph/9710335].
- [45] F. Borzumati and C. Greub, Phys. Rev. D **58**, 074004 (1998) doi:10.1103/PhysRevD.58.074004 [hep-ph/9802391].
- [46] C. Bobeth, M. Misiak and J. Urban, Nucl. Phys. B **567**, 153 (2000) doi:10.1016/S0550-3213(99)00688-4 [hep-ph/9904413].
- [47] P. Gambino and M. Misiak, Nucl. Phys. B **611**, 338 (2001) doi:10.1016/S0550-3213(01)00347-9 [hep-ph/0104034].
- [48] M. Misiak *et al.*, Phys. Rev. Lett. **114**, no. 22, 221801 (2015) doi:10.1103/PhysRevLett.114.221801 [arXiv:1503.01789 [hep-ph]].
- [49] M. Misiak and M. Steinhauser, Eur. Phys. J. C **77**, no. 3, 201 (2017) doi:10.1140/epjc/s10052-017-4776-y [arXiv:1702.04571 [hep-ph]].

- [50] G. Aad *et al.* [ATLAS Collaboration], Phys. Rev. D **91**, no. 11, 112011 (2015) doi:10.1103/PhysRevD.91.112011 [arXiv:1503.05425 [hep-ex]].
- [51] G. Aad *et al.* [ATLAS Collaboration], JHEP **1508**, 105 (2015) doi:10.1007/JHEP08(2015)105 [arXiv:1505.04306 [hep-ex]].
- [52] G. Aad *et al.* [ATLAS Collaboration], JHEP **1602**, 110 (2016) doi:10.1007/JHEP02(2016)110 [arXiv:1510.02664 [hep-ex]].
- [53] G. Aad *et al.* [ATLAS Collaboration], Eur. Phys. J. C **76**, no. 8, 442 (2016) doi:10.1140/epjc/s10052-016-4281-8 [arXiv:1602.05606 [hep-ex]].
- [54] G. Aad *et al.* [ATLAS Collaboration], Phys. Lett. B **758**, 249 (2016) doi:10.1016/j.physletb.2016.04.061 [arXiv:1602.06034 [hep-ex]].
- [55] M. Aaboud *et al.* [ATLAS Collaboration], JHEP **1708**, 052 (2017) doi:10.1007/JHEP08(2017)052 [arXiv:1705.10751 [hep-ex]].
- [56] M. Aaboud *et al.* [ATLAS Collaboration], JHEP **1710**, 141 (2017) doi:10.1007/JHEP10(2017)141 [arXiv:1707.03347 [hep-ex]].
- [57] M. Aaboud *et al.* [ATLAS Collaboration], JHEP **1807**, 089 (2018) doi:10.1007/JHEP07(2018)089 [arXiv:1803.09678 [hep-ex]].
- [58] M. Aaboud *et al.* [ATLAS Collaboration], arXiv:1806.01762 [hep-ex].
- [59] M. Aaboud *et al.* [ATLAS Collaboration], arXiv:1806.10555 [hep-ex].
- [60] M. Aaboud *et al.* [ATLAS Collaboration], arXiv:1808.01771 [hep-ex].
- [61] M. Aaboud *et al.* [ATLAS Collaboration], arXiv:1808.02343 [hep-ex].
- [62] S. Chatrchyan *et al.* [CMS Collaboration], Phys. Rev. Lett. **112**, no. 17, 171801 (2014) doi:10.1103/PhysRevLett.112.171801 [arXiv:1312.2391 [hep-ex]].
- [63] V. Khachatryan *et al.* [CMS Collaboration], Phys. Rev. D **93**, no. 11, 112009 (2016) doi:10.1103/PhysRevD.93.112009 [arXiv:1507.07129 [hep-ex]].
- [64] V. Khachatryan *et al.* [CMS Collaboration], Phys. Rev. D **93**, no. 1, 012003 (2016) doi:10.1103/PhysRevD.93.012003 [arXiv:1509.04177 [hep-ex]].
- [65] V. Khachatryan *et al.* [CMS Collaboration], Phys. Lett. B **771**, 80 (2017) doi:10.1016/j.physletb.2017.05.019 [arXiv:1612.00999 [hep-ex]].
- [66] A. M. Sirunyan *et al.* [CMS Collaboration], JHEP **1704**, 136 (2017) doi:10.1007/JHEP04(2017)136 [arXiv:1612.05336 [hep-ex]].
- [67] A. M. Sirunyan *et al.* [CMS Collaboration], JHEP **1705**, 029 (2017) doi:10.1007/JHEP05(2017)029 [arXiv:1701.07409 [hep-ex]].
- [68] A. M. Sirunyan *et al.* [CMS Collaboration], Phys. Lett. B **772**, 634 (2017) doi:10.1016/j.physletb.2017.07.022 [arXiv:1701.08328 [hep-ex]].
- [69] A. M. Sirunyan *et al.* [CMS Collaboration], JHEP **1711**, 085 (2017) doi:10.1007/JHEP11(2017)085 [arXiv:1706.03408 [hep-ex]].
- [70] A. M. Sirunyan *et al.* [CMS Collaboration], Phys. Lett. B **781**, 574 (2018) doi:10.1016/j.physletb.2018.04.036 [arXiv:1708.01062 [hep-ex]].
- [71] A. Spiezia [CMS Collaboration], arXiv:1708.03124 [hep-ex].
- [72] A. Djouadi, Phys. Rept. **457**, 1 (2008) doi:10.1016/j.physrep.2007.10.004 [hep-ph/0503172].

- [73] G. Aad *et al.* [ATLAS and CMS Collaborations], JHEP **1608**, 045 (2016) doi:10.1007/JHEP08(2016)045 [arXiv:1606.02266 [hep-ex]].
- [74] G. Aad *et al.* [ATLAS Collaboration], Phys. Rev. D **92**, no. 11, 112007 (2015) doi:10.1103/PhysRevD.92.112007 [arXiv:1509.04261 [hep-ex]].
- [75] R. Dermisek, J. P. Hall, E. Lunghi and S. Shin, JHEP **1412**, 013 (2014) doi:10.1007/JHEP12(2014)013 [arXiv:1408.3123 [hep-ph]].
- [76] A. Falkowski, D. M. Straub and A. Vicente, JHEP **1405**, 092 (2014) doi:10.1007/JHEP05(2014)092 [arXiv:1312.5329 [hep-ph]].
- [77] M. Aaboud *et al.* [ATLAS Collaboration], [arXiv:1807.07915 [hep-ex]].
- [78] M. E. Peskin and T. Takeuchi, Phys. Rev. D **46**, 381 (1992). doi:10.1103/PhysRevD.46.381
- [79] R. Barbieri, A. Pomarol, R. Rattazzi and A. Strumia, Nucl. Phys. B **703**, 127 (2004) doi:10.1016/j.nuclphysb.2004.10.014 [hep-ph/0405040].
- [80] M. Tanabashi *et al.* [Particle Data Group], Phys. Rev. D **98**, no. 3, 030001 (2018). doi:10.1103/PhysRevD.98.030001
- [81] G. Cynolter and E. Lendvai, Eur. Phys. J. C **58**, 463 (2008) doi:10.1140/epjc/s10052-008-0771-7 [arXiv:0804.4080 [hep-ph]].
- [82] M. Capdequi Peyranere, H. E. Haber and P. Irulegui, Phys. Rev. D **44**, 191 (1991). doi:10.1103/PhysRevD.44.191
- [83] R. D. Ball *et al.* [NNPDF Collaboration], JHEP **1504**, 040 (2015) doi:10.1007/JHEP04(2015)040 [arXiv:1410.8849 [hep-ph]].
- [84] M. Czakon and A. Mitov, Comput. Phys. Commun. **185**, 2930 (2014) doi:10.1016/j.cpc.2014.06.021 [arXiv:1112.5675 [hep-ph]].
- [85] N. Kidonakis, JHEP **0505**, 011 (2005) doi:10.1088/1126-6708/2005/05/011 [hep-ph/0412422].
- [86] S. h. Zhu, Phys. Rev. D **67**, 075006 (2003) doi:10.1103/PhysRevD.67.075006 [hep-ph/0112109].
- [87] T. Plehn, Phys. Rev. D **67**, 014018 (2003) doi:10.1103/PhysRevD.67.014018 [hep-ph/0206121].
- [88] E. L. Berger, T. Han, J. Jiang and T. Plehn, Phys. Rev. D **71**, 115012 (2005) doi:10.1103/PhysRevD.71.115012 [hep-ph/0312286].
- [89] S. S. D. Willenbrock, Phys. Rev. D **35**, 173 (1987). doi:10.1103/PhysRevD.35.173
- [90] M. Spira, hep-ph/9510347.
- [91] N. Kidonakis, PoS DIS **2015**, 170 (2015) doi:10.22323/1.247.0170 [arXiv:1506.04072 [hep-ph]].
- [92] J. Alwall *et al.*, JHEP **1407**, 079 (2014) doi:10.1007/JHEP07(2014)079 [arXiv:1405.0301 [hep-ph]].
- [93] G. Aad *et al.* [ATLAS Collaboration], Phys. Lett. B **716**, 142 (2012) doi:10.1016/j.physletb.2012.08.011 [arXiv:1205.5764 [hep-ex]].
- [94] S. Chatrchyan *et al.* [CMS Collaboration], Phys. Rev. Lett. **110**, 022003 (2013) doi:10.1103/PhysRevLett.110.022003 [arXiv:1209.3489 [hep-ex]].

- [95] M. Aaboud *et al.* [ATLAS Collaboration], [arXiv:1812.09743 [hep-ex]].
- [96] Priyanka *et al.* [CMS Collaboration], arXiv:1901.04179 [hep-ex].
- [97] T. Hahn and M. Perez-Victoria, *Comput. Phys. Commun.* **118**, 153 (1999)  
doi:10.1016/S0010-4655(98)00173-8 [hep-ph/9807565].